Articles

Pyrazole Ligands: Structure−Affinity/Activity Relationships and Estrogen Receptor-α-Selective Agonists

Shaun R. Stauffer,[†] Christopher J. Coletta,[†] Rosanna Tedesco,[†] Gisele Nishiguchi,[†] Kathryn Carlson,[†] Jun Sun,[‡] Benita S. Katzenellenbogen,[‡,#] and John A. Katzenellenbogen*[,†]

Departments of Chemistry, Physiology, and Cell and Structural Biology, University of Illinois and University of Illinois College of Medicine, Urbana, Illinois 61801

Received June 9, 2000

We have found that certain tetrasubstituted pyrazoles are high-affinity ligands for the estrogen receptor (ER) (Fink et al. *Chem. Biol.* **1999**, *6*, 205−219) and that one pyrazole is considerably more potent as an agonist on the ERα than on the ER*β* subtype (Sun et al. *Endocrinology* **1999**, *140*, 800−804). To investigate what substituent pattern provides optimal ER binding affinity and the greatest enhancement of potency as an ERα-selective agonist, we prepared a number of tetrasubstituted pyrazole analogues with defined variations at certain substituent positions. Analysis of their binding affinity pattern shows that a C(4)-propyl substituent is optimal and that a *p*-hydroxyl group on the N(1)-phenyl group also enhances affinity and selectivity for ERα. The best compound in this series, a propylpyrazole triol (PPT, compound **4g**), binds to ERα with high affinity (ca. 50% that of estradiol), and it has a 410-fold binding affinity preference for ERα. It also activates gene transcription only through ERα. Thus, this compound represents the first *ERα-specific agonist*. We investigated the molecular basis for the exceptional ERα binding affinity and potency selectivity of pyrazole **4g** by a further study of structure−affinity relationships in this series and by molecular modeling. These investigations suggest that the pyrazole triols prefer to bind to ERα with their C(3)-phenol in the estradiol A-ring binding pocket and that binding selectivity results from differences in the interaction of the pyrazole core and C(4)-propyl group with portions of the receptor where ERα has a smaller residue than ER*β*. These ER subtype-specific interactions and the ER subtype-selective ligands that can be derived from them should prove useful in defining those biological activities in estrogen target cells that can be selectively activated through ERα.

Introduction

The estrogen receptor (ER) displays a remarkable capacity for binding nonsteroidal ligands with high affinity.[1] Many of these ligands have been developed into hormonal agents having mixed agonist−antagonist and tissue-selective activities that are useful in menopausal hormone replacement, in fertility regulation, and in the prevention and treatment of breast cancer. Because of their unusual pharmacology, some of these agents have been termed **s**elective **e**strogen **r**eceptor **m**odulators (SERMs).[2] To understand the molecular basis of the tissue selectivity of these SERMs, it would be helpful to know in detail how they are interacting with the ER. However, short of performing X-ray crystallographic analysis of ER complexes with each ligand, it can be a challenge to obtain such information.

If the nonsteroidal ligand bears a reasonable structural relationship with steroidal estrogens, it is generally quite easy to imagine the orientation that this ligand is likely to adopt when it is bound by ER.[3,4] ER mutagenesis studies,[5] and the recent X-ray crystallographic structures of ER complexed with both estradiol and three nonsteroidal ligands (raloxifene, hydroxytamoxifen, and diethylstilbestrol), provide additional guidance in the selection of reasonable binding orientations for ligands of this type.[4,6] However, when the nonsteroidal estrogens have structures that are more divergent from those of steroidal estrogens, it becomes a greater challenge to predict ligand-binding orientation.[7]

The recent characterization of a second ER gene, encoding ER*β*, places a further premium on our understanding of the details of ligand−receptor interaction,[8,9] because it would be especially interesting to have ligands that could activate or inhibit each of the ER subtypes with high selectivity. Such ligands would be valuable tools to define the biological effects that are mediated by ERα and ER*β*. So far, however, there have been only a few reports of ER subtype-selective estrogens, and in many cases, the selectivity has been relatively modest.[10]

Recently, we investigated various heterocyclic diazole structures as core elements for nonsteroidal estrogens

* Address correspondence to: John A. Katzenellenbogen, Dept. of Chemistry, University of Illinois, 600 S. Mathews Ave., Urbana, IL 61801. Tel: 217-333-6310. Fax: 217-333-7325. E-mail: jkatzene@uiuc.edu.
[†] Department of Chemistry.
[‡] Department of Physiology.
[#] Department of Cell and Structural Biology.

10.1021/jm000170m CCC: $19.00
Published on Web 11/28/2000

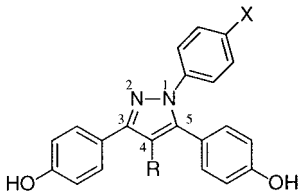

Figure 1. Pyrazole core optimized for high-affinity ER binding (X = H, OH; R = alkyl).

of novel design.[11,12] Our aim was to identify systems that would be amenable to combinatorial assembly and library synthesis. From among the several systems we studied that included imidazoles, oxazoles, thiazoles, and isoxazoles, we found that high-affinity ER ligands could be obtained by appropriate substitution on a pyrazole core. Subsequently, we used a parallel, solid-phase synthesis approach to prepare some combinatorial pyrazole libraries of moderate size.[13] In the cases we investigated, high-affinity binding required tetrasubstitution of the pyrazole core and an appropriate display of aromatic, phenolic, and aliphatic groups.[11,12] An example of this optimal pattern of substitution that we have thus far delineated for pyrazoles includes three aromatic groups at the 1-, 3-, and 5-positions, specifically phenols at the 3- and 5-positions, and an alkyl group at the 4-position (Figure 1). Initial studies on one of these compounds (Figure 1; X = H, R = Et) showed that it acted as an agonist on both ER subtypes, but it was considerably more potent on ERα than on ERβ.[14] Thus, this pyrazole was termed an ERα potency-selective agonist.[14]

In this report, we have investigated structure−activity relationships in these tetrasubstituted pyrazoles to delineate two aspects of their behavior: (1) the C(4)-alkyl substituent and phenol hydroxyl pattern that provide optimal ER subtype selectivity and (2) the extent to which the ERα-selective binding affinity and potency of these pyrazoles can be understood in the context of crystal structures of the ERα ligand-binding domain (LBD) and models for ERβ derived from these structures. Our studies provide new information on these issues, and in the process, we have identified a pyrazole that shows complete ERα selectivity in transcription activation by the receptor.

Results and Discussion

Chemical Syntheses. The compounds we have studied have various C(4)-alkyl substituents and have either a phenyl or 4-hydroxylphenyl substituent on N(1). Shown in Scheme 1 is the route used for the synthesis of the pyrazoles **4a**−**i**. The starting alkylphenones **1a**−**f** were readily prepared in good yields by Friedel−Crafts acylation of anisole. The requisite β-diketones **2a**−**e** were then produced in moderate to good yields by acylation of the corresponding lithium enolates with 4-nitrophenyl 4-methoxybenzoate. Because the pyrazoles are sterically crowded, rather harsh conditions were required for their formation (>16 h at reflux at 110−120 °C in DMF/THF solution). Nonetheless, these conditions served quite well for pyrazole formation in solution. Several of the pyrazole intermediates protected as methyl ethers were isolated in good yield. However, with the trimethoxy pyrazoles **3g**−**i**, it was difficult to separate the protected product from traces of the diketone precursor by chromatography. So, in these cases the crude material was passed through a short silica gel column and, without further purification, was then deprotected using BBr_3. Pyrazoles **3d**,**e** were also treated in this manner. The final phenolic pyrazoles **4a**−**i** were isolated in 30−98% yield after purification by recrystallization and/or chromatography.

Scheme 1. Synthesis of C(4)-Alkylpyrazole Analogues

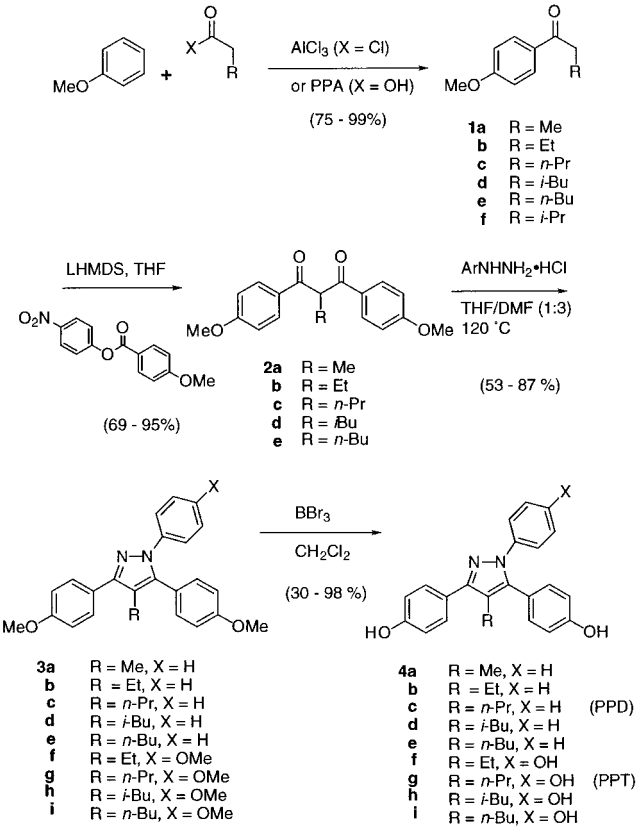

In addition to the final pyrazole products **4a**−**i**, we wished to prepare the isopropyl analogue derived from ketone **1f**. However, we encountered difficulties in the preparation of this hindered dione because of significant O-acylation that occurred during the Claisen condensation. Separation of the O-acylated byproduct from the desired dione proved to be difficult. Moreover, once the dione was isolated, the pyrazole condensation failed using the conditions described above, which had been optimized for solution-phase synthesis. To avoid these problems, we utilized a solid-phase synthesis according to the methodology that we had previously developed,[13] and in this manner we were able to obtain the isopropylpyrazole **6** starting from the resin-bound ketone **5**, as shown in Scheme 2, although the overall yield was relatively low.

To prepare a complete series of all of the possible diphenol and monophenol analogues of the C(4)-ethyl triphenol **4f**, we also synthesized monophenols **7a**−**c** and the remaining diphenols **8a**,**b** (all mono- and diphenols are shown in Scheme 3, top). Monophenol **7a** was prepared from dibenzoylmethane (**9**) and 4-methoxyphenylhydrazine by the usual sequence[11] (Scheme 3, middle). The synthesis of the remaining two monophenols (**7b**,**c**) by a regioselective route has been described elsewhere (not shown).[15] The two remaining

Scheme 2. Synthesis of C(4)-Isopropylpyrazole **6** by Solid-Phase Methodology[13]

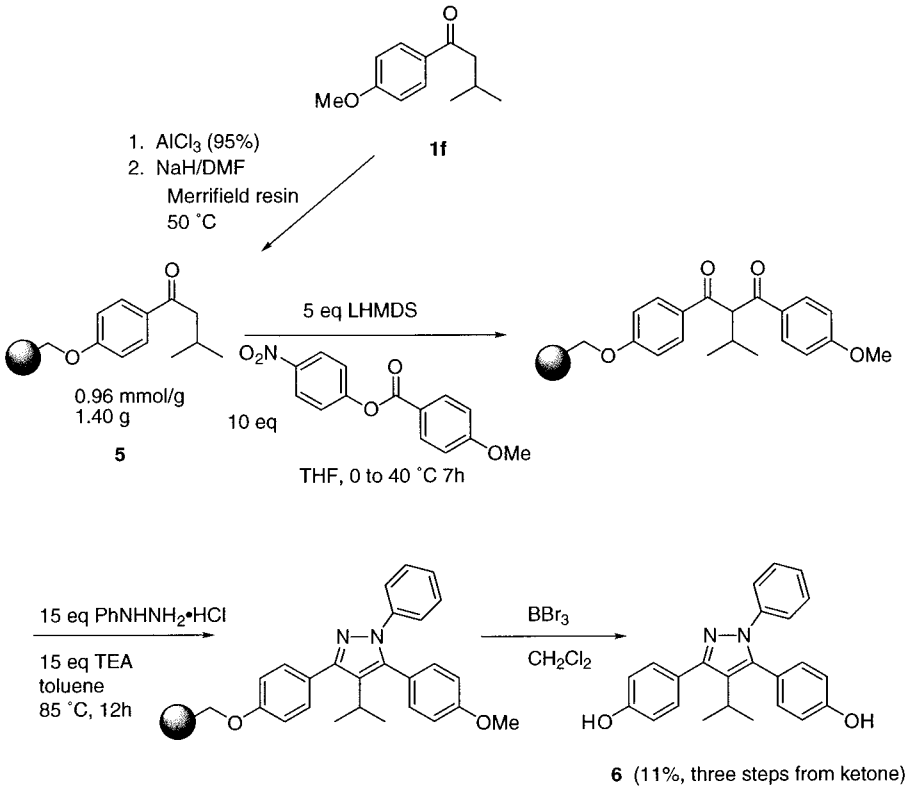

diphenols (**8a**,**b**) were also prepared by this regioselective method, as shown in Scheme 3 (bottom). The two chalcones (**12a**,**b**) are treated with *p*-methoxyphenylhydrazine under anerobic conditions to give the pyrazolines **13a**,**b**. The corresponding anions, generated by treatment with LDA, were ethylated, and the C(4)-ethylpyrazolines **14a**,**b** were then oxidized to the pyrazoles **15a**,**b** and deprotected to the desired bisphenols **8a**,**b**.

ER Binding Affinity of Tetrasubstituted Pyrazoles. The ER binding affinity of pyrazoles **4a**−**i**, **6**, **7a**−**c**, and **8a**,**b** was determined in a competitive radiometric binding assay using purified full-length human ERα and ERβ, as previously described.[16,17] The affinities are expressed as relative binding affinity (RBA) values and are presented in two tables: Table 1, which is discussed here, covers the effect of the nature of the C(4)-alkyl substituent on the binding affinity and ER subtype selectivity of pyrazoles in the triphenol and the principal 3,5-diphenol series; the data in Table 2, which compares the affinity of the three possible mono- and diphenols with the triphenol in the C(4)-ethylpyrazole series, relates to the issue of ligand orientation and is discussed in a later section.

Two interesting trends are notable in the binding affinity data presented in Table 1. In both the diphenol series (X = H, **4a**−**e**, **6**) and the triphenol series (X = OH, **4f**−**i**), optimal binding affinity for ERα requires a C(4)-alkyl substituent that is not too long (*n*-Bu: **4e**,**i**) or too short (Me: **4a**), the highest affinity being found with the intermediate size substituents: Et (**4b**,**f**), *n*-Pr (**4c**,**g**), and *i*-Bu (**4d**,**h**). Thus, it appears that the subpocket that is accommodating this group has a limited size and relatively narrow shape. A more significant trend evident in this series has to do with the effect of the phenolic substituent on the N(1)-phenyl group. In each case where a comparison can be made (namely, Et, Pr, *i*-Bu, or *n*-Bu), the triphenols (X = OH, **4f**−**i**) have higher affinity on ERα and/or lower affinity on ERβ than do the diphenols (X = H, **4a**−**e**). As a result, the triphenols consistently have higher ERα affinity selectivity than do the corresponding 3,5-diphenols.[18] In fact, some of the members show a remarkable selectivity in their binding affinity for ERα vs ERβ, which is 30−40 for some of the pyrazole diols (**4c**,**d**) and as high as 200−400 for some of the pyrazole triols (**4f**,**g**).

The increased ERα binding affinity of the triphenols is not expected, because additional polar substituents are generally poorly tolerated in the center of the ligand-binding pocket of ER, at least in most nonsteroidal ligand systems that have been examined, such as the benzo[*b*]thiophenes[19] and 2,3-diarylindans.[7] One exception is found with certain triphenylacrylonitriles, where addition of a third hydroxyl increases binding affinity.[20]

We have previously reported binding affinities for one of these pyrazoles (**4b**), using receptor preparations containing only the *LBDs* of human ERα and ERβ, rather than *full-length* human ERα and ERβ.[14] The values obtained previously were higher but less ERα-selective (60 ± 16 for ERα and 18 ± 4 for ERβ). At this point, the reasons for these affinity differences between full-length ER and the ER LBD are not clear, although they have been seen, as well, in a structurally different class of ER ligands.[17] However, it is of note that the higher ERα/ERβ affinity ratio that we obtain for pyrazole **4b** with the full-length ERs is more consistent with the 120-fold potency ratio we described in transcription assays than was the 3-fold ERα/ERβ affinity ratio obtained with ERs containing only the LBDs.[14]

Transcriptional Activity and Potency of Tetra-

Scheme 3. Synthesis of the Remaining Mono- and Diphenolic C(4)-Ethylpyrazoles

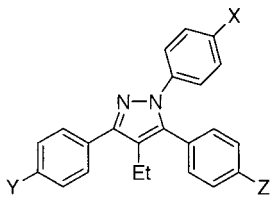

		X	Y	Z
Monophenols:	**7a**	OH	H	H
	7b	H	OH	H
	7c	H	H	OH
Diphenols:	**4b**	H	OH	OH
	8a	OH	H	OH
	8b	OH	OH	H

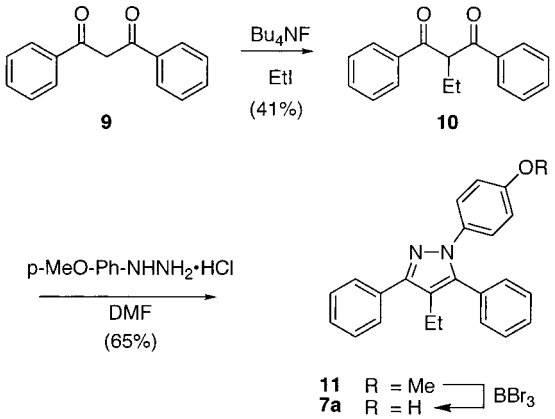

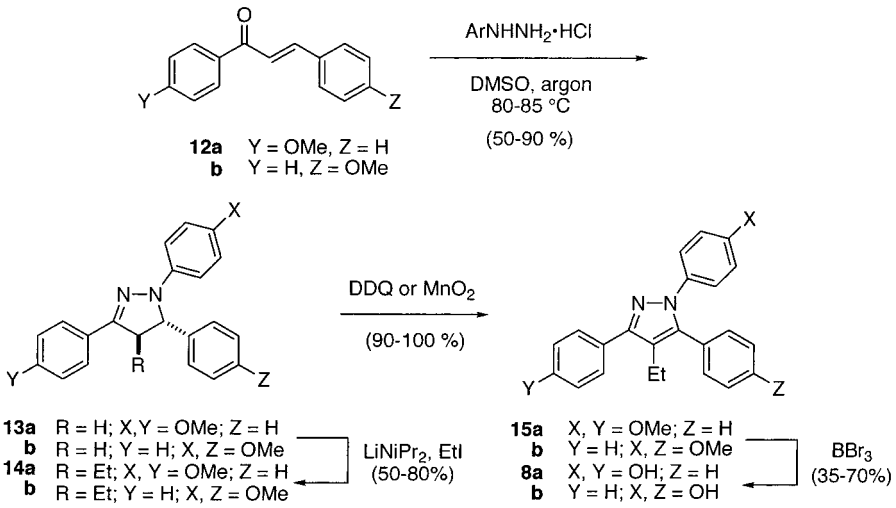

substituted Pyrazoles. For investigation of transcription activation ability, we selected two compounds: the pyrazole having the highest ERα/ERβ affinity selectivity (410-fold, the propylpyrazole triol **4g**, called PPT for convenience) and the corresponding pyrazole in the diol series (**4c**, called propylpyrazole diol or PPD). These two pyrazoles were assayed for estrogen agonist activity in transactivation assays using human endometrial cancer (HEC-1) cells transfected with expression plasmids for ERα and ERβ and an estrogen-responsive reporter gene plasmid. The dose−response curves for these compounds are shown in Figure 2.

Both compounds are potent in activating gene transcription through ERα, but the PPD (**4c**) is weak in transcriptional activation through ERβ and PPT (**4g**) is completely inactive in stimulating transcription via ERβ. Thus, PPT (**4g**) is an ERα-specific agonist. This pharmacological profile is reminiscent of the behavior of the C(4)-ethyl analogue of pyrazole **4c** (namely, pyrazole **4b**), that we have previously described as an agonist that is more potent on ERα than on ERβ. This compound (**4b**) had an EC_{50} of ca. 1 nM on ERα and showed a 120-fold potency selectivity for this ER subtype.[14] However, in cell transfection assays both PPT and PPD are nearly 10-fold more potent than the original pyrazole **4b** on ERα, and they are much more ERα-selective.

As we had noted in our earlier study on pyrazole **4b**,[14] and is clearly evident here as well, the ERα selectivity of these pyrazoles in terms of their *potency* in transcription assays is substantially greater than their *affinity* selectivity in binding assays. For example, the ERα affinity selectivity of PPD (**4c**) is 32, yet its potency selectivity is ca. 1000 (cf. Figure 2). Likewise, the ERα affinity selectivity of PPT (**4g**) is 410, and its potency selectivity, which although is difficult to accurately evaluate (cf. Figure 2), is probably greater than 10000. Such a discordance between affinity and potency might be explained in the context of "tripartite receptor pharmacology", a concept that we advanced some time

Table 1. Relative Binding Affinity Data for C(4)-Alkyl Triphenol and 3,5-Diphenol Pyrazole Analogues[a]

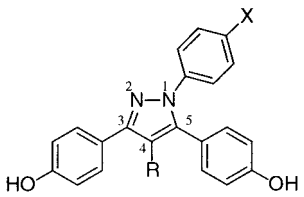

compd	R	X	RBA ERα[b]	RBA ERβ[b]	ERα/ERβ RBA ratio
			3,5-Diphenols		
4a	Me	H	0.76 ± 0.18	0.28 ± 0.16	2.7
4b	Et	H	31 ± 15	1.1 ± 0.2	28
6	*i*-Pr	H	5.6 ± 2	0.86 ± 0.11	6.5
4c (PPD)	*n*-Pr	H	16.8 ± 0.3	0.52 ± 0.03	32
4d	*i*-Bu	H	56 ± 6	1.4 ± 0	40
4e	*n*-Bu	H	8.7 ± 2.0	0.47 ± 0.1	19
			1,3,5-Triphenols		
4f	Et	OH	36 ± 6	0.15 ± 0.014	240
4g (PPT)	*n*-Pr	OH	49 ± 12	0.12 ± 0.04	410
4h	*i*-Bu	OH	75 ± 6	0.89 ± 0.06	84
4i	*n*-Bu	OH	14 ± 4	0.18 ± 0.09	77

[a] Relative binding affinity (RBA), where estradiol is 100%. Values are the mean of at least 2 and more typically 3 or more independent determinations (±SD).[33] [b] Competitive radiometric binding assays were done with purified full-length human ERα and ERβ (PanVera Inc.), using 10 nM [^{3}H]E_2 as tracer and HAP for adsorption of the receptor−tracer complex.[16,17]

ago.[21] Binding measured in vitro with purified ERs involves only the interaction between ligand and receptor, whereas transcription measured in cells involves the additional interaction of the ligand−receptor complex with coactivators and other cellular components. Thus, compared to their relative affinities for ERα and ERβ, the relative potency of two ligands can be modulated by differences in the strength with which their respective ligand−receptor complexes bind to coactivators or are modified by other cellular elements, although other factors, as well, might be involved. In this case, it appears that the pyrazole complexes with ERα are better able to bind coactivators than are the ERβ−pyrazole complexes, as we have documented in a recent study.[22]

A Model for the Binding of Pyrazoles with the ER Subtypes. The high affinity, and particularly the high selectivity, with which these pyrazoles bind to ERα raises the important issue of what molecular features underlie the differences in their interaction with ERα vs ERβ. Without crystal structures available for the comparison of any of these pyrazoles complexed with both ERα and ERβ, we are currently limited to investigating this issue by molecular modeling.

1. Structure−Affinity Relationships and the Orientation of Pyrazoles in the Ligand-Binding Pocket of ERα. Because the pyrazoles we have studied here are rather symmetrical and are polyphenolic, it is not obvious which orientation these ligands might prefer to adopt within the ligand-binding pocket of ER. In principle, the triphenolic pyrazoles could adopt six orientations (see Figure 4): Each of the three phenolic rings could play the role of the A-ring of estradiol, and in each case the remainder of the pyrazole could adopt two orientations about the bond connecting the A-ring phenol mimic to the pyrazole core (darkened bond). These six binding modes are given the designations: N(1), N(1)′, C(3), C(3)′, C(5), and C(5)′.

A classical approach that has been used to try to ascertain which orientation di- and triphenolic compounds adopt within the ER binding pocket has been to systematically delete the phenolic hydroxyl group and examine the effect of this deletion on the binding affinity.[7] Because the hydroxy group on the phenol that corresponds to the A-ring of estradiol is thought to make the major contribution to ligand-binding affinity, the greatest reduction in binding should occur when this hydroxyl group is the one deleted.[3] We have undertaken such an analysis by comparing the affinities of pyrazoles in which the three phenols in the triphenol **4f** were each singly deleted (diphenol set: **4b**, **8a**,**b**) or were deleted in three pairs (monophenol set: **7a**−**c**). The affinities of these three diphenols and three monophenols, together with the triphenol parent **4f**, are listed in Table 2. Because we had prepared the most pyrazoles in the C(4)-ethyl series, we chose to do this structure−affinity study in this series.

The simplest analysis we can make of the structure−binding affinity pattern shown in Table 2 is the following: In the monophenol set (**7a**−**c**), the N(1)- and C(3)-phenols (**7a**,**b**) have comparable affinities, but the C(5)-phenol (**7c**) binds ca. 100-fold less well. Because of the very low affinity of the C(5)-monophenol (**7c**), we believe that the C(5)-phenol cannot function as the mimic of the A-ring of estradiol, in essence, eliminating orientations C(5) and C(5)′ as possibilities. (It is of note that these two "eliminated" binding modes project bulky groups simultaneously in directions that correspond to C(7) and C(11) of estradiol; cf. Figure 3.) Elimination of the C(5)-phenol leaves the N(1)- and C(3)-phenols as potential estradiol A-ring mimics, but the very similar affinities of both of these monophenols suggest that each one may function as the A-ring mimic.

Analysis of the binding affinity pattern of the bisphenols is somewhat more ambiguous, but suggestive, nevertheless: Deletion of the N(1)-phenol from the triphenol has only a minor effect on the binding affinity (**4b** vs triphenol **4f**), which means that in the context of the triphenol in ERα, the N(1)-phenol is not contributing significantly to binding affinity. Thus, one would expect that the C(3)-phenol is likely to be the more important of the two and thus that the orientations C(3) and C(3)′ are more likely than the orientations N(1) and N(1)′. Deletion of either the C(3)-phenol or the C(5)-phenol results in a 4−5-fold decrease in binding (**8a**,**b** vs **4f**). The fact that the N(1),C(3)-bisphenol (**8b**) still binds quite well is not surprising, because the C(3)-phenol is still available to be the estradiol A-ring mimic. However, the fact that the N(1),C(5)-phenol (**8a**) also binds quite well might seem surprising, because this diphenol lacks the important C(3)-hydroxyl.

We believe that the reasonably good affinity of diphenol **8a** suggests that this pyrazole can bind with the N(1) group as the estradiol A-ring mimic, meaning that the N(1) and N(1)′ ligand orientations are also possible, though, based on the minimal effect of the N(1)-phenol deletion, they are probably not significantly populated when a C(3)-phenol is available. (It seems unlikely that diphenol **8a** would bind with the C(5)-phenol in the A-ring pocket, because of the very low affinity of the

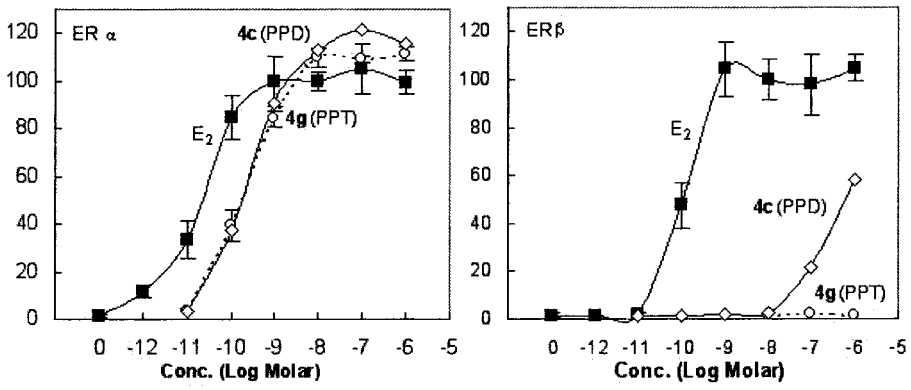

Figure 2. Transcription activation by ERα (left) and ERβ (right) in response to pyrazoles **4c** (PPD) and **4g** (PPT). Human endometrial cancer (HEC-1) cells were transfected with expression vectors for ERα or ERβ and an (ERE)3-pS2-CAT reporter gene and were treated with the indicated concentrations of ligand for 24 h. CAT activity was normalized for β-galactosidase activity from an internal control plasmid. Values are expressed as a percent of the ERα or ERβ response with 1 nM E_2, which is set at 100%.[32]

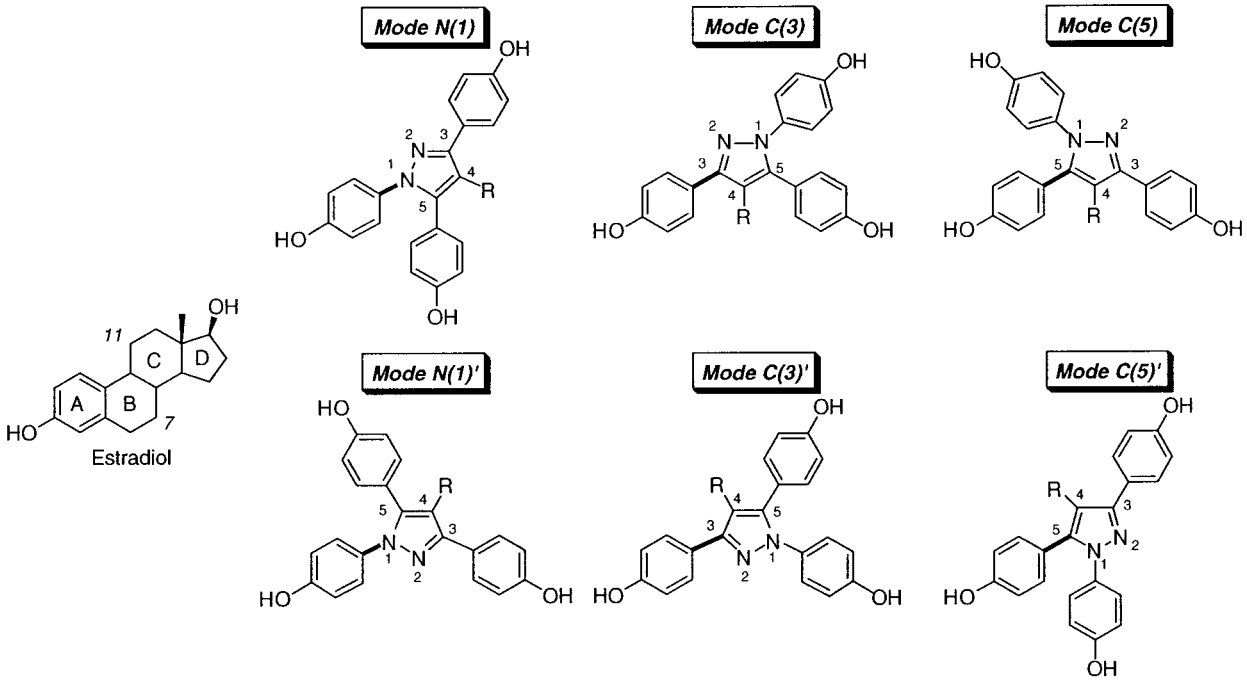

Figure 3. Potential pyrazole binding relative to estradiol. Both modes A and A′ have the C(3)-phenol oriented to project in to the estradiol A-ring binding pocket. Modes A and A′ are related to one another by rotation of the pyrazole core around the darkened bond.

C(5)-monophenol **7c**.) Thus, the phenol deletion/binding affinity approach has only reduced the number of possible ligand orientations in the binding pocket from six to four, with a suggested preference for two orientations, C(3) and C(3)′. As described in the section below, we have tried to narrow down the possible ligand orientations even further by molecular modeling.

The conclusions thus far that the C(3)-phenol is the preferred A-ring mimic but that the N(1)-phenol is a possible alternative are consistent with two other studies that we have recently completed. In a related but more limited investigation of the orientation of ligand binding in two isomeric pyrazole series, we concluded that the orientation with the C(3)-phenol as the A-ring mimic was most likely in the pyrazole series that is the same as the one studied here and that in the isomeric series the phenol that occupied topologically congruent substituent position also functioned as the A-ring mimic.[23] In another investigation in which we worked to convert these pyrazoles from agonists to antagonists by appending a basic side chain onto the four substituents on these pyrazoles, we found that high affinity was retained only when this group was attached to the C(5)-hydroxyl.[24] On the basis of this structure−affinity pattern, as well as some molecular modeling and consideration of the structure of the ER LBD complexes with antagonists, we concluded in that study that the most likely orientation of these basic side chain-substituted pyrazoles was N(1).[24] In this orientation, the basic side chain could project outward through the 11β-channel that forms in the ER LBD complexes with antagonists.[4,6]

2. Molecular Modeling of the Orientation of Pyrazole Triols in the Ligand-Binding Pocket of the ERs. We have previously done modeling of the pyrazole ligands in the ER LBDs, first in our initial study on these ligands[11] and, more recently, in connection with a study of the orientation of these ligands in

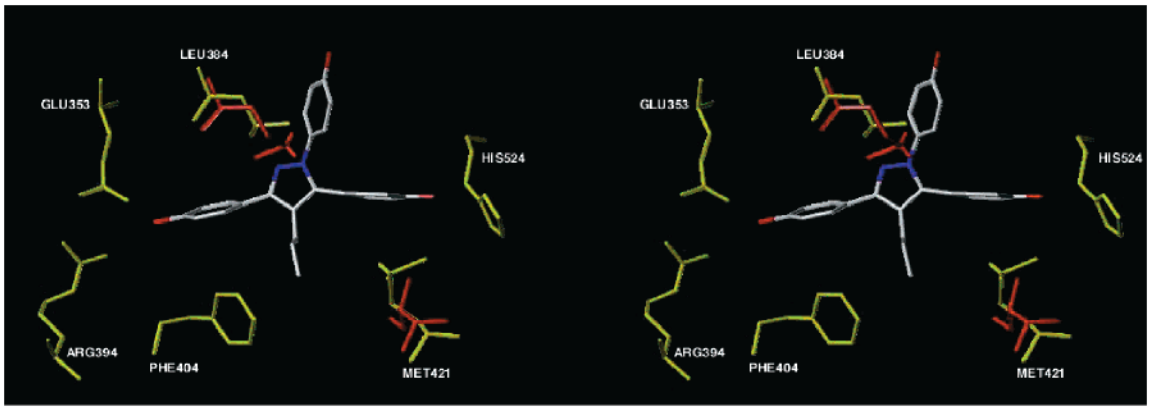

Figure 4. Crossed-stereoview of propylpyrazole triol (PPT, **4g**) docked and minimized in ERα LBD pocket according to binding mode A, showing selected residues close to the ligand. The pyrazole ligand is shown with standard atom colors. The residues in ERα are identified and shown in yellow. At the two positions where the ERβ sequence differs from ERα, the ERβ residues are shown in red (Met in ERβ in place of ERα Leu384 and Ile in ERβ in place of ERα Met421).

Table 2. Relative Binding Affinity Data for C(4)-Ethylpyrazole Tri-, Di-, and Monophenols[a]

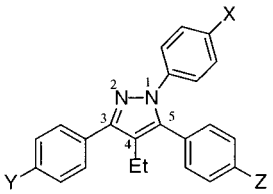

compd	X N(1)	Y C(3)	Z C(5)	RBA ERα[b]	RBA ERβ[b]	ERα/ERβ RBA ratio
				Monophenols		
7a	OH	H	H	3.1 ± 0.5	1.5 ± 0.2	2.1
7b	H	OH	H	2.6 ± 0.1	0.61 ± 0.2	4.3
7c	H	H	OH	0.04 ± 0.11	0.06 ± 0.01	0.67
				Diphenols		
4b	H	OH	OH	31 ± 15	1.1 ± 0.2	28
8a	OH	H	OH	7.0 ± 0.6	0.80 ± 0.09	9
8b	OH	OH	H	8.9 ± 0.6	0.32 ± 0.01	28
				Triphenols		
4f	OH	OH	OH	36 ± 6	0.15 ± 0.014	240

[a] Relative binding affinity (RBA), where estradiol is 100%. Values are the mean of at least 2 and more typically 3 or more independent determinations (±SD).[33] [b] Competitive radiometric binding assays were done with purified full-length human ERα and ERβ (PanVera Inc.), using 10 nM [^{3}H]E_2 as tracer and HAP for adsorption of the receptor−tracer complex.[16,17]

the binding pocket.[23] As a result of this latter study,[23] we have come to appreciate that there are some ambiguities in how polyphenolic ligands such as these pyrazoles might be accommodated by ER, at least at the level at which we are currently able to model. Such ambiguity is echoed in the results of the structure−binding affinity considerations discussed above. Therefore, for the purposes of this paper, we have chosen to illustrate a binding mode for these pyrazoles in which the C(3)-phenyl group is placed in the ER LBD pocket that normally binds the A-ring of estradiol (Figure 3, see C(3) and C(3)′), as this appeared to be the most likely orientation for these polyphenolic systems (see above and ref 23). We have, however, also examined the other four possible orientations.

We conducted a ligand docking/binding minimization routine by placing PPT (**4g**) in ERα in both orientations: mode C(3) and mode C(3)′ (Flexidock routine within Sybyl; see Experimental Section, Molecular Modeling). During the course of the ligand docking routine, the PPT that began in orientation mode C(3)′ became reoriented into mode C(3), whereas the one that began in mode C(3) remained in mode C(3). Therefore, mode C(3)′ was not considered further. After the docking/minimization routine, the PPT in mode C(3) was nicely accommodated in this orientation, with only minimal changes in the side chain conformations of some of the residues that line the ligand-binding pocket. We also modeled the four other possible orientations of this pyrazole using the same routine (not shown), but we found that none of them gave a fit as good as that of the pyrazole orientation illustrated as mode C(3) in Figure 3. The fact that the N(1) and N(1)′ modes did not score well in our modeling, although they seemed possible on the basis of the structure−affinity considerations above, suggests either limitations in our modeling method or the fact that these modes are not important in the triphenolic pyrazoles and only become important when certain phenols are missing (see above) or a basic side chain is appended.[24]

In Figure 4, we show a crossed-stereoview skeletal model illustrating PPT (**4g**) in the ERα structure, oriented in binding mode C(3), after the ligand docking/minimization routine. For clarity and for the ERα and ERβ comparison below, only selected residues from ER are shown. In this orientation, the N(1)-phenyl group of PPT (**4g**) projects into a region of the binding pocket which represents the C/D-subpocket that is normally occupied by portions of the C- and D-rings and the 18-methyl substituent on estradiol (E_2). Despite the importance of the N(1)-phenol in enhancing ERα binding selectivity (see above and Table 1), there are no obvious sites for its interaction in this subpocket. The N(1)- and C(5)-aryl groups of PPT project somewhat more deeply into the C/D-subpocket than do the corresponding regions of estradiol. However, this region is known to tolerate a variety of substituents,[3] and certain residues have been repositioned by the docking/minimization routine to make additional space for the pyrazole ligand. It is of note that these residue conformational changes, which allow for PPT binding in this mode, involve relatively minimal alteration in the total protein energy.

3. Analysis of Interactions Between Pyrazole Substituents and Amino Acid Residues in ERα and ERβ. We have used the C(3) orientation mode

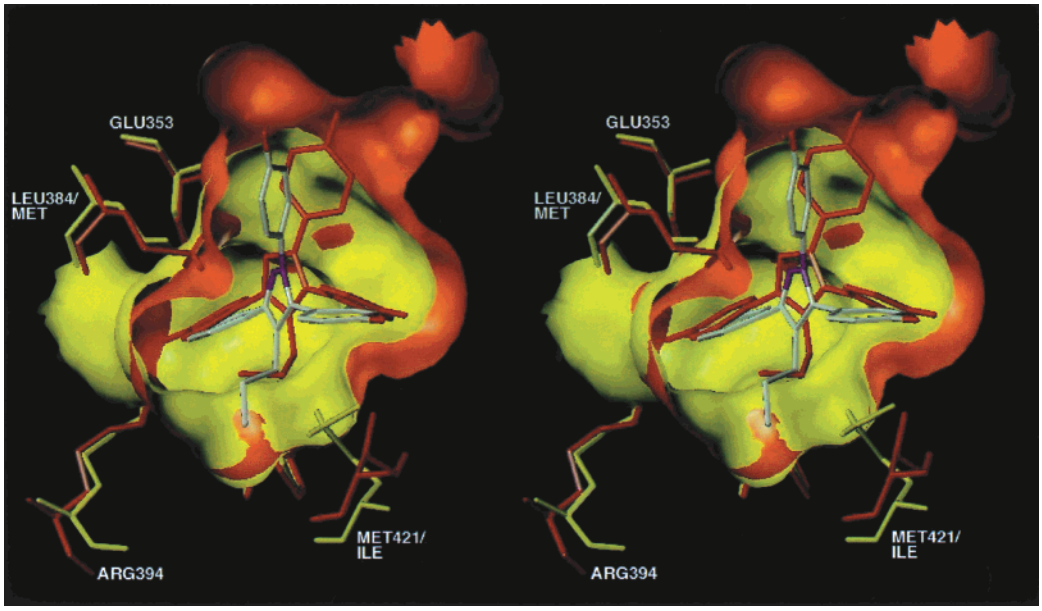

Figure 5. Crossed-stereoview of ligand skeletal structures and receptor molecular surfaces for the ERα− and ERβ−propylpyrazole triol (PPT, **4g**) complexes. The PPT in ERα is shown with standard atom colors, and the ERα receptor surface is shown in yellow; in the ERβ−PPT complex, both the ligand and receptor surface are shown in red. For further details, see text.

model derived above to try to understand the origins of the high ERα affinity selectivity of PPT (**4g**), and to do this, we have constructed a model for ERβ that is derived from ERα LBD−diethylstilbestrol (DES) structure (see Experimental Section for details).[6] Although the LBDs of ERα and ERβ have only 56% amino acid identity, the residues that line the ligand-binding pocket are nearly identical.[25] In fact, of the 22−24 residues that are considered to be in contact with the ligand (i.e., within 4 Å), all but two are identical in ERα and ERβ.[25] The only differences are at ERα position 384, where ERα has a leucine but ERβ has a methionine, and at ERα position 421, where ERα has a methionine but ERβ has an isoleucine. It has been speculated that these sequence differences, in particular, may underlie the differences in the ERα and ERβ binding affinities of ligands that have been studied so far.[25] For clarity, we have distinguished these residues in Figure 4 by color: The residues common to ERα and ERβ are illustrated in yellow, but at the two positions where the ERβ residues are different, the ERβ residues, colored in red, are superimposed over the ERα residues in yellow (see Figure 4 and legend).

In this model with the most ERα potency-selective ligand PPT (**4g**), we can see that the pyrazole core itself has the closest contact with Leu384 in the case of ERα and Met384 in the case of ERβ. For the Met/Ile discriminating residues at ERα position 421, the C(4)-propyl group as well as the C(5)-aryl group appear to have close contacts, although this interaction seems less severe.

A model for PPT (**4g**) binding to ERβ was generated by changing the two residues in the ERα ligand-binding pocket to those found in ERβ, inserting the ligand according to mode C(3), and then conducting the ligand docking/minimization routine as was done before with ERα (see Experimental Section). The comparative fit of this pyrazole in the ligand-binding pocket of ERα and ERβ can be appreciated by the composite receptor surface model shown in Figure 5 in crossed-stereoview. In this figure, we have displayed the pyrazoles in both of the receptors as skeletal structures, and the two pockets as colored surfaces. The ligand in the ERα model is shown with standard atom colors and the ERα surface in yellow; both the ligand and receptor in the ERβ model are shown in red. In this figure, the view has been rotated, twisting the C(3)-phenol away from the viewer; this orientation is the best we have found to display differences between the two models.

The principal difference in the surface of the ligand-binding pocket is at the site where ERα has a smaller residue (Leu384) than ERβ (Met384). This is illustrated by the sharp red interpenetrating surface in the middle left region of the pocket. The increased steric bulk in ERβ at this site makes contact with the pyrazole core of this ligand, displacing it relative to the pyrazole position in the ERα model. Because the C(3)-phenol remains relatively fixed in the rather rigid A-ring binding pocket, this pyrazole core displacement causes a large shift in the position of the N(1)-phenol and a significant but somewhat smaller shift of the C(5)-phenol and the propyl group. The large shift of the N(1)-phenol is intriguing, because this group contributes significantly to the ERα affinity and potency selectivity of these pyrazoles. However, we have been unable to identify any interaction in the N(1)-phenol subpocket that would favor the presence of a hydroxyl in ERα and disfavor it in ERβ.

The shift of the propyl group forces this substituent to adopt a gauche conformation in ERβ (vs an anti orientation in ERα); this is a change that would most likely increase ligand internal energy and reduce binding affinity. The shift of the pyrazole position in the ERβ model moves the C(5)-phenol toward the site where the smaller Ile residue in ERβ replaces the bulkier Met421 in ERα. Thus, the different shape of the ligand-binding pocket in ERβ, in particular the increased bulk of the ERβ Met residue where ERα has a Leu, appears to interfere with the optimal binding of the pyrazole ligand and is therefore thought to account for its lowered

binding affinity. It is interesting to note that even after extensive minimization, there is a substantial energy difference between the two complexes, with the ERα complex having greater stabilization by ca. 30 kcal/mol.

Conclusions

A series of C(4)-alkyl tetrasubstituted pyrazole analogues have been prepared and their RBA values determined for the ER. These compounds show an interesting binding affinity pattern, including high-affinity selectivity for ERα, which for the propylpyrazole triol (PPT, **4g**) reaches 410-fold. This compound also has very high potency selectivity for ERα in reporter gene transcription assays in cells, and it is the first ERα-specific agonist. Structure−affinity relationships in a series of mono-, di-, and triphenolic pyrazoles and molecular modeling suggests that these pyrazoles bind to the ER with the C(3)-phenol in the A-ring binding pocket. A model of PPT (**4g**) docked in the ERα LBD−DES crystal structure in the most likely binding orientation suggests that the very high ERα binding selectivity of this pyrazole derives from particular interactions between the pyrazole core and the C(4)-propyl group with a region on the ligand-binding pocket where ERα has a smaller residue (Leu384) than ERβ (Met384). These interactions may serve as the basis for future structure-based design of ERα- and ERβ-specific ligands.

Experimental Methods

General. All reagents and solvents were obtained from Aldrich, Fisher, or Mallinckrodt. Tetrahydrofuran was freshly distilled from sodium/benzophenone. Dimethylformamide was vacuum distilled prior to use and stored over 4 Å molecular sieves. Melting points were determined on a Thomas-Hoover UniMelt capillary apparatus and are uncorrected. All reactions were performed under a dry N_2 atmosphere unless otherwise specified. Reaction progress was monitored by analytical thin-layer chromatography using GF silica plates purchased from Analtech. Visualization was achieved by short-wave UV light (254 nm) or potassium permanganate stain. Radial preparative-layer chromatography was performed on a Chromatotron instrument (Harrison Research, Inc., Palo Alto, CA) using EM Science silica gel Kieselgel 60 PF_{254} as adsorbent. Flash column chromatography was performed using Woelm 32−63 μm silica gel packing.[26] Synthetic procedures for **1a**−**f** and spectral data for **1d**,**f** are described below. Compounds **1a**,[27] **1b**,[28] **1c**,[29] and **1e**[30] were spectroscopically identical to the reported compounds. The synthesis of compounds **7b**,**c** has been described elsewhere.[15]

^{1}H and ^{13}C NMR spectra were recorded on either a Varian Unity 400 or 500 MHz spectrometers using $CDCl_3$ or MeOD-d_4 as solvent. Chemical shifts are reported as parts per million downfield from an internal tetramethylsilane standard (δ 0.0 for ^{1}H) or from solvent references. NMR coupling constants are reported in hertz (Hz). ^{13}C NMR were determined using either the attached proton test (APT) or standard ^{13}C pulse sequence parameters. Low- and high-resolution electron impact mass spectra were obtained on Finnigan MAT CH-5 or 70-VSE spectrometers. Low- and high-resolution fast atom bombardment (FAB) were obtained on a VG ZAB-SE spectrometer. Elemental analyses were performed by the Microanalytical Service Laboratory of the University of Illinois. Those final components that did not give satisfactory combustion analysis (i.e., **4b**−**d**, **6**, **8a**) gave satisfactory exact mass determinations and were found to be at least 98% pure by HPLC analysis under normal and reversed-phase conditions.

RBA Assays. Purified ERα and ERβ binding affinities were determined using a competitive radiometric binding assay using 10 nM [^{3}H]estradiol as tracer, commercially available ERα and ERβ preparations (PanVera Inc., Madison, WI), and hydroxylapatite (HAP) to adsorb bound receptor−ligand complex.[16,17] HAP was prepared following the recommendations of Williams and Gorski.[31] All incubations were done at 0 °C for 18−24 h. Binding affinities are expressed relative to estradiol (RBA = 100%) and are reproducible with a coefficient of variation of 0.3.

Transcription Activation Assays. Human endometrial cancer (HEC-1) cells were maintained in culture and transfected as described previously.[32] Transfection of HEC-1 cells in 60-mm dishes used 0.4 mL of a calcium phosphate precipitate containing 2.5 μg of pCMVβGal as internal control, 2 μg of the reporter gene plasmid, 100 ng of the ER expression vector, and carrier DNA to a total of 5 μg DNA. CAT activity, normalized for the internal control β-galactosidase activity, was assayed as previously described.[32]

Molecular Modeling for Pyrazole 4g. The starting conformation for **4g** used for receptor docking studies was generated from a random conformational search performed using the MMFF94 force field as implemented in Sybyl 6.6. The resulting lowest-energy conformer was then used for docking studies. Charge calculations were determined using the MMFF94 method and molecular surface properties displayed using MOLCAD module in Sybyl 6.6.

Pyrazole **4g**, generated as noted above, was prepositioned in the DES−ERα LBD crystal structure (Protein Data Bank code 3ERD)[6] using a least-squares multifitting of select atoms within the DES ligand. Once prepositioned, DES was deleted and ligand **4g** optimally docked in the ERα binding pocket using the Flexidock routine within Sybyl (Tripos). Both hydrogen-bond donors and acceptors within the pocket surrounding the ligand (Glu353, Arg394, and His524), the ligand itself, and select torsional bonds were defined. The best docked receptor−ligand complex from Flexidock then underwent a three-step minimization: first nonring torsional bonds of the ligand were minimized in the context of the receptor using the torsmin command, followed by minimization of the side chain residues within 8 Å of the ligand while holding the backbone and residues Glu353 and Arg394 fixed. A final third minimization of both the ligand and receptor was conducted using the Anneal function (hot radius 8 Å, interesting radius 16 Å from pyrazole **4g**) to afford the final model.

The ERβ molecular model was generated within Sybyl by first modifying residues Leu384 to Met384 and Met421 to Ile421 in the DES−ERα LBD crystal structure[6] and conducting an initial minimization of these two residues while holding the remaining atoms fixed. This was followed by a final minimization using the Anneal function (hot radius 4 Å, interesting radius 8 Å from Met384 and Ile421) using conditions similar to above. The pyrazole **4g** was introduced into this ERβ model and the Flexidock routine implemented as for the ERα model (see above). All minimizations were done using the MMFF94 force field with the Powell gradient method (final rms < 0.02 kcal/mol·Å).

Chemical Syntheses. General Procedure for Preparation of Alkylphenones Using $AlCl_3$ (1a−c,f): Method A. To a stirred solution of $AlCl_3$ (46.8 mmol) in 1,2-dichloroethane (10 mL) at 0 °C was added the commercial acid chloride (39.0 mmol) dropwise over 10 min. The resulting solution was allowed to come to room temperature for 20 min until all of the $AlCl_3$ had dissolved. The reaction mixture was cooled to 0 °C and a solution of anisole (5.1 mL, 46.8 mmol) in 1,2-dichloroethane (20 mL) was then added dropwise over 30 min. Upon completion, the reaction was allowed to reach room temperature and stir for 8−15 h. The mixture was then quenched by pouring over 100 g of ice and extracted with CH_2Cl_2 (3 × 25 mL). The combined organic layers were washed with water, $NaHCO_3$ (satd), brine, then dried over $MgSO_4$ and concentrated under reduced pressure. Excess anisole was removed in vacuo and then the ketone product distilled.

General Procedure for Preparation of Alkylphenones Using PPA (1d,e): Method B. A mechanically stirred mixture consisting of carboxylic acid (1.0 equiv), anisole (1.1 equiv) and polyphosphoric acid (PPA; 6.15 g/mL of anisole) was heated to 90−100 °C for 1.5 h. Upon cooling to near room

temperature, the dark mixture was poured over ice (100 g/0.1 mol) and extracted repeatedly with EtOAc. The organic layers were then washed with satd $NaHCO_3$ followed by brine. After drying the extract over Na_2SO_4 and removal of solvent, a crude oil was obtained. The final products were purified by bulb-to-bulb distillation.

1-(4-Methoxyphenyl)-4-methylpentan-1-one (1d). Prepared according to method B outlined above to afford the title compound as a pale yellow oil (75%): ^{1}H NMR ($CDCl_3$, 500 MHz) δ 0.94 (d, 6H, $J = 6.0$), 1.60 (m, 3H, overlapping methine and β-CH_2), 2.90 (t, 2H, $J = 6.8$), 3.87 (s, 3H), 6.92 (d, 2H, $J = 8.8$), 7.90 (d, 2H, $J = 8.8$); ^{13}C NMR ($CDCl_3$, 125 MHz) δ 22.6, 28.5, 33.9, 36.4, 55.2, 113.5, 130.2, 163.6, 198.7; MS (EI, 70 eV) m/z 206.1 (M^+). Anal. ($C_{13}H_{18}O_2$) C, H.

1-(4-Methoxyphenyl)-3-methylbutan-1-one (1f). Prepared according to general method A outlined above to afford the title compound as a pale yellow oil (84%): ^{1}H NMR ($CDCl_3$, 500 MHz) δ 0.95 (d, 6H, $J = 6.7$), 2.24 (sept, 1H, $J = 6.6$), 2.73 (d, 2H, $J = 6.7$), 3.81 (s, 3H), 6.88 (d, 2H, $J = 8.9$), 7.90 (d, 2H, $J = 9.2$); ^{13}C NMR ($CDCl_3$, 125 MHz) δ 22.6, 25.2, 46.2, 55.2, 113.5, 130.2, 130.3, 163.1, 198.7; HRMS (EI, M^+) calcd for $C_{12}H_{16}O_2$ 192.1150, found 192.1153.

2-Methyl-1,3-bis(4-methoxyphenyl)propane-1,3-dione (2a). To a solution of **1a** (160 mg, 0.97 mmol) and 4-nitrophenyl 4-methoxybenzoate (prepared from *p*-nitrophenol and 4-methoxybenzoic acid using diisopropylcarbodiimide and 4-(dimethyamino)pyridine in THF (35 mL) at 0 °C was added a 1.0 M solution of lithium hexamethyldisilamide (3.03 mL, 3.03 mmol) dropwise over 5 min. The reaction was warmed to room temperature and allowed to stir for 1.5 h. At this time the reaction was quenched by the addition of H_2O (25 mL). The mixture was then repeatedly extracted with diethyl ether. The organic layers were combined and washed with H_2O, then dried over Na_2SO_4 and concentrated under reduced pressure to afford a crude solid. Unreacted ester was removed by adding a solution of 40% ethyl acetate/hexanes and filtering off the insoluble ester. The remaining filtrate was concentrated and subjected to flash chromatography (40% ethyl acetate/hexanes) to afford the title compound as a light yellow oil (266 mg, 92%): ^{1}H NMR ($CDCl_3$, 500 MHz) δ 1.58 (d, 3H, $J = 7.3$), 3.85 (s, 3H), 5.13 (q, 1H, $J = 7.2$), 6.92 (d, 2H, $J = 6.8$), 7.93 (d, 2H, $J = 7.0$).

2-Ethyl-1,3-bis(4-methoxyphenyl)propane-1,3-dione (2b).[11] Prepared according to the procedure outlined above from **1b** and purified by flash chromatography (ethyl acetate/hexanes) to afford a viscious oil (95%): ^{1}H NMR ($CDCl_3$, 500 MHz) δ 1.01 (t, 3H, $J = 7.4$), 2.12 (quint, 2H, $J = 7.1$), 3.80 (s, 6H), 4.98 (t, 1H, $J = 6.6$), 6.87 (AA′XX′, 2H, $J = 8.8$, 2.1), 7.94 (AA′XX′, 2H, $J = 8.5$, 2.3); APT ^{13}C NMR ($CDCl_3$, 125 MHz) δ 12.9 (CH_3), 23.2 (CH_2), 55.6 (CH), 58.8 (CH_3O), 114.0 (ArCH), 129.3 (ArC), 131.0 (ArCH), 163.8 (ArC), 195.0 (C=O); MS (EI, 70 eV) m/z 312.3 (M^+).

2-Propyl-1,3-bis(4-methoxyphenyl)propane-1,3-dione (2c). Prepared according to the procedure outlined above from **1c** and purified by flash chromatography (ethyl acetate/hexanes) to afford product as a clear viscous oil (76%): ^{1}H NMR (CDCl3, 500 MHz) δ 0.95 (t, 3H, $J = 7.4$), 1.36−1.47 (m, 2H), 2.06−2.11 (m, 2H), 3.83 (s, 6H), 5.05 (t, 1H, $J = 6.7$) 6.90 (AA′XX′, 2H, $J = 9.0$, 2.5), 7.95 (AA′XX′, 2H, $J = 9.0$, 2.5); ^{13}C NMR ($CDCl_3$, 125 MHz) δ 14.0, 21.5, 31.6, 55.4, 57.1, 113.8, 129.0, 130.8, 163.5, 194.8; HRMS (EI, M^+) calcd for $C_{20}H_{22}O_4$ 326.1518, found 326.1512.

2-Isobutyl-1,3-bis(4-methoxyphenyl)propane-1,3-dione (2d). Prepared according to the procedure outlined above from **1d** and purified by flash chromatography (ethyl acetate/hexanes) to afford product as a clear viscous oil (77%): ^{1}H NMR ($CDCl_3$, 500 MHz) δ 0.96 (d, 3H, $J = 6.5$), 1.70 (m, 1H, $J = 6.7$), 2.00 (br t, 2H, $J = 6.9$), 3.82 (s, 6H), 5.18 (t, 1H, $J = 6.5$), 6.89 (d, 2H, $J = 8.6$), 7.97 (d, 2H, $J = 9.0$); ^{13}C NMR ($CDCl_3$, 125 MHz) δ 22.8 (CH_3), 27.2 (CH), 38.5 (CH_2), 55.7 (CH_3O), 55.8 (CH), 114.2 (ArCH), 129.4 (ArC), 131.2 (ArCH), 163.2 (C=O); HRMS (EI, M^+) calcd for $C_{13}H_{18}O_4$ 340.1674, found 340.1679. Anal. ($C_{21}H_{24}O_4$) C, H.

2-*n*-Butyl-1,3-bis(4-methoxyphenyl)propane-1,3-dione (2e). Prepared according to the procedure outlined above from **1e** and purified by flash chromatography (ethyl acetate/hexanes) to afford product as a light yellow oil (69%): ^{1}H NMR ($CDCl_3$, 500 MHz) δ 0.89 (t, 3H, $J = 7.0$), 1.37 (m, 4H), 2.11 (q, 2H, $J = 7.1$), 3.85 (s, 6H), 6.91 (d, 4H, $J = 9.0$), 7.98 (d, 4H, $J = 9.0$); ^{13}C NMR ($CDCl_3$, 125 MHz) δ 14.0 (CH_3), 22.9 (CH_2), 22.7 (CH_2), 30.7 (CH_2), 55.7 (CH_3O), 57.7 (CH), 114.2 (ArCH), 129.5 (ArC), 131.2 (ArCH), 163.2 (C=O); HRMS (EI, M^+) calcd for $C_{13}H_{18}O_4$ 340.1674, found 340.1675. Anal. ($C_{13}H_{18}O_4$) C, H.

General Procedure for Pyrazole Synthesis. To a DMF (30 mL) and THF (10 mL) solution containing diketone (1.0 mmol) was added phenylhydrazine hydrochloride (3−5 equiv). The mixture was brought to reflux (oil bath temperature 120 °C) until disappearance of diketone as evident by TLC analysis (8−20 h). The reaction mixture was then allowed to cool to room temperature and diluted with H_2O (30 mL). The product was extracted repeatedly with ethyl acetate (3 × 25 mL) and the organic layers combined and washed sequentially with a satd LiCl solution (25 mL), satd $NaHCO_3$ (25 mL), and brine (25 mL). The oganic layer was dried over Na_2SO_4 and concentrated under reduced pressure to afford the crude product in the form of an oil, which was purified by flash chromatography or by passage through a short silica plug eluting with an ethyl acetate/hexane solvent system.

3,5-Bis(4-methoxyphenyl)-4-methyl-1-phenyl-1*H*-pyrazole (3a). The diketone **2a** (250 mg, 0.84 mmol) was reacted with phenylhydrazine hydrochloride (423 mg, 2.94 mmol) according to the general procedure above. Upon purification by flash chromatography (40% ethyl acetate/hexanes) the title compound was obtained as a tan solid (220 mg, 71%): mp 142−143 °C; ^{1}H NMR ($CDCl_3$, 500 MHz) δ 2.21 (s, 3H), 3.83 (s, 3H), 3.86 (s, 3H), 6.89 (AA′XX′, 2H, $J = 8.9$, 2.5), 6.99 (AA′XX′, 2H, $J = 8.9$, 2.5), 7.15 (AA′XX′, 2H, $J = 8.8$, 2.5), 7.19−7.32 (m, 5H), 7.74 (AA′XX′, 2H, $J = 8.9$, 2.5); ^{13}C NMR ($CDCl_3$, 125 MHz) δ 10.2, 55.2, 55.3, 113.6, 113.9, 113.9, 123.1, 124.7, 126.5, 126.6, 128.7, 129.1, 131.3, 140.4, 141.2, 150.9, 159.2, 159.4; MS (EI, 70 eV) m/z 370 (M^+). Anal. ($C_{24}H_{22}N_2O_2$) C, H, N.

4-Ethyl-3,5-bis(4-methoxyphenyl)-1-phenyl-1*H*-pyrazole (3b).[11] Diketone **2b** and phenylhydrazine hydrochloride were reacted as outlined above to afford **3b** as an orange solid after flash chromatography purification (87%): ^{1}H NMR ($CDCl_3$, 400 MHz) δ 1.04 (t, 3H, $J = 7.6$), 2.63 (q, 2H, $J = 7.6$), 3.83 (s, 3H), 3.86 (s, 3H), 6.90 (AA′XX′, 2H, $J = 8.8$, 2.4), 6.99 (AA′XX′, 2H, $J = 8.8$, 2.6), 7.17 (AA′XX′, 2H, $J = 8.8$, 2.4), 7.20 (m, 2H), 7.24 (m, 3H), 7.72 (AA′XX′, 2H, $J = 9.0$, 2.4); ^{13}C NMR ($CDCl_3$, 100 MHz) δ 15.8, 17.3, 55.4, 55.5, 114.1, 114.2, 120.7, 123.5, 124.8, 126.8, 127.0, 128.8, 129.3, 131.5, 140.5, 141.2, 150.8, 159.4, 159.6; HRMS (EI, M^+) calcd for $C_{25}H_{24}N_2O_2$ 384.1835, found 384.1837.

3,5-Bis(4-methoxyphenyl)-1-phenyl-4-propyl-1*H*-pyrazole (3c). Diketone **2c** (200 mg, 0.61 mmol) was reacted with phenylhydrazine hydrochloride (444 mg, 3.07 mmol) according to the general procedure to afford **3c** as an orange oil (130 mg, 53%) after purification by flash chromatography (40% ethyl acetate/hexanes): ^{1}H NMR ($CDCl_3$, 500 MHz) δ 0.79 (t, 3H, $J = 7.4$), 1.42 (sext, 2H, $J = 7.7$), 2.57 (t, 2H, $J = 8.0$), 3.83 (s, 3H), 3.86 (s, 3H), 6.90 (AA′XX′, 2H, $J = 8.6$, 2.5), 6.99 (AA′XX′, 2H, $J = 8.8$, 2.5), 7.18−7.32 (m, 5H), 7.15 (AA′XX′, 2H, $J = 8.6$, 2.5), 7.72 (AA′XX′, 2H, $J = 8.8$, 2.5); ^{13}C NMR ($CDCl_3$, 125 MHz) δ 14.05, 23.79, 25.86, 55.09, 55.15, 113.74, 113.85, 118.87, 118.86, 122.86, 124.60, 126.52, 129.49, 131.17, 139.66, 141.31, 150.36, 159.14, 159.33; HRMS (EI, M^+) calcd for $C_{26}H_{26}N_2O_2$ 398.1994, found 398.2000.

4-Isobutyl-3,5-bis(4-methoxyphenyl)-1-phenyl-1*H*-pyrazole (3d). Diketone **2d** was reacted with phenylhydrazine hydrochloride according to the general procedure to afford **3d** as an orange oil (85%) after a short silica plug (20% ethyl acetate/hexanes). The purified material was then directly used in the subsequent deprotection step.

4-Butyl-3,5-bis(4-methoxyphenyl)-1-phenyl-1*H*-pyrazole (3e). Diketone **2e** was reacted with phenylhydrazine hydrochloride according to the general procedure to afford **3e** as a reddish oil (86%) after purification by flash chromatog-

raphy (20% ethyl acetate/hexanes). This material was then directly used in the subsequent deprotection step.

4-Ethyl-1,3,5-tris(4-methoxyphenyl)-1*H*-pyrazole (3f). Diketone **2b** (400 mg, 1.28 mmol) was reacted with 4-methoxyphenylhydrazine hydrochloride (1.11 g, 6.40 mmol) according to the general procedure. The crude product was purified by flash chromatography (2% acetone/CH_2Cl_2) to afford **3f** as an oil (351 mg, 66%): ^{1}H NMR ($CDCl_3$, 500 MHz) δ 1.06 (t, 3H, J = 7.5), 2.65 (q, 2H, J = 7.5), 3.73 (s, 3H), 3.79 (s, 3H), 3.83 (s, 3H), 6.78 (AA′XX′, 2H, J = 9.0, 2.8) 6.89 (AA′XX′, 2H, J = 8.8, 2.4), 6.69 (AA′XX′, 2H, J = 8.8, 2.4), 7.16 (AA′XX′, 2H, J = 8.8, 2.4), 7.21 (AA′XX′, 2H, J = 9.0, 2.7), 7.74 (AA′XX′, 2H, J = 8.7, 2.4); ^{13}C NMR ($CDCl_3$, 125 MHz) δ 15.52, 17.09, 55.05, 55.10, 55.22, 113.65, 113.80, 113.83, 119.78, 123.11, 125.96, 126.78, 128.95, 131.18, 133.45, 140.84, 149.94, 158.99, 157.97, 159.22; HRMS (EI, M^+) calcd for $C_{26}H_{26}N_2O_3$ 414.1943, found 414.1942.

1,3,5-Tris(4-methoxyphenyl)-4-propyl-1*H*-pyrazole (3g). Diketone **2c** (500 mg, 1.52 mmol) was reacted with 4-methoxyphenylhydrazine hydrochloride (800 mg, 4.59 mmol) according to the general procedure to afford 362 mg of **3g** as a red oil (67%) after a short silica plug (20% ethyl acetate/hexanes). This material was then directly used in the subsequent deprotection step.

4-Isobutyl-1,3,5-tris(4-methoxyphenyl)-1*H*-pyrazole (3h). Diketone **2d** was reacted with 4-methoxyphenylhydrazine hydrochloride according to the general procedure to afford **3h** as a light orange oil (85%) after a short silica plug (20% ethyl acetate/hexanes). The purified material was then directly used in the subsequent deprotection step.

4-Butyl-1,3,5-tris(4-methoxyphenyl)-1*H*-pyrazole (3i). Diketone **2e** was reacted with 4-methoxyphenylhydrazine hydrochloride according to the general procedure to afford **3i** as a light orange oil (87%) after a short silica plug (20% ethyl acetate/hexanes). The purified material was then directly used in the subsequent deprotection step.

General Demethylation Procedure. To a stirred solution of methyl-protected pyrazole (1 equiv) in CH_2Cl_2 at −78 °C was added dropwise a 1 M BBr_3 solution in CH_2Cl_2 (3−5 equiv). Upon complete addition of BBr_3, the reaction was maintained at −78 °C for 1 h and then allowed to reach room temperature and stir for an additional 16 h. The mixture was cooled to 0 °C and carefully quenched with H_2O (15−25 mL). The product was then repeatedly extracted with EtOAc and the organic layers dried over Na_2SO_4. Upon solvent removal the crude phenolic products were purified by flash chromatography and/or recrystallization from MeOH/CH_2Cl_2 mixtures.

3,5-Bis(4-hydroxyphenyl)-4-methyl-1-phenyl-1*H*-pyrazole (4a). A stirred CH_2Cl_2 solution of **3a** (200 mg, 0.54 mmol) was deprotected using BBr_3 according to the general demethylation procedure. Purification by flash chromatography (5% CH_3OH/CH_2Cl_2) afforded the title compound as a tan solid (54 mg, 30%): mp 225−230 °C; ^{1}H NMR (MeOD-d_4, 500 MHz) δ 2.13 (s, 3H), 6.76 (AA′XX′, 2H, J = 8.4, 2.7), 6.93 (AA′XX′, 2H, J = 8.7, 2.5), 7.01 (AA′XX′, 2H, J = 8.8, 2.5), 7.54 (AA′XX′, 2H, J = 8.6, 2.4), 7.35−7.22 (m, 5H); ^{13}C NMR (MeOD-d_4, 125 MHz) 8.7, 112.8, 114.7, 114.8, 120.9, 124.4, 124.8, 126.7, 128.3, 128.9, 130.9, 139.8, 151.4, 157.1, 157.4; MS (EI, 70 eV) m/z 342. Anal. ($C_{22}H_{18}N_2O_2 \cdot H_2O$) C, H, N.

4-Ethyl-3,5-bis(4-hydroxyphenyl)-1-phenyl-1*H*-pyrazole (4b).[11] A stirred CH_2Cl_2 solution of **3b** (100 mg, 0.26 mmol) was deprotected using BBr_3 according to the general demethylation procedure. Purification by flash chromatography (5% CH_3OH/CH_2Cl_2) afforded the title compound as a white solid (50 mg, 54%): mp 247−248 °C; ^{1}H NMR (MeOD-d_4, 400 MHz) δ 0.98 (t, 3H, J = 7.4), 2.60 (q, 2H, J = 7.5), 6.78 (AA′XX′, 2H, J = 8.8, 2.4), 6.88 (AA′XX′, 2H, J = 8.7, 2.5), 7.05 (AA′XX′, 2H, J = 8.8, 2.4), 7.24−7.42 (m, 5H), 7.51 (AA′XX′, 2H, J = 8.7, 2.5); HRMS (EI, M^+) calcd for $C_{23}H_{21}N_2O_2$ 357.1611, found 357.1603.

3,5-Bis(4-hydroxyphenyl)-1-phenyl-4-propyl-1*H*-pyrazole (4c). A stirred CH_2Cl_2 solution of **3c** (107 mg, 0.27 mmol) was deprotected using BBr_3 according to the general demethylation procedure. The crude product was purified by flash chromatography (10% CH_3OH/CH_2Cl_2) to afford **4c** as a tan solid (85 mg, 86%): mp 240−245 °C; ^{1}H NMR (MeOD-d_4, 500 MHz) δ 0.72 (t, 3H, J = 7.4), 1.35 (sext, 2H, J = 7.5), 2.55 (t, 2H, J = 7.7), 6.77 (AA′XX′, 2H, J = 8.7, 2.5), 6.88 (AA′XX′, 2H, J = 8.5, 2.4), 7.03 (AA′XX′, 2H, J = 8.5, 2.4), 7.32−7.27 (m, 5H), 7.50 (AA′XX′, 2H, J = 8.8, 2.5); ^{13}C NMR (MeOD-d_4, 400 MHz) δ 12.73, 13.28, 25.28, 114.75, 114.89, 118.26, 121.13, 124.78, 124.82, 126.69, 128.26, 128.99, 131.02, 139.71, 142.12, 151.30, 157.08, 157.49; HRMS (EI, M^+) calcd for $C_{24}H_{22}N_2O_2$ 370.1681, found 370.1676.

4-Isobutyl-3,5-bis(4-hydroxyphenyl)-1-phenyl-1*H*-pyrazole (4d). A stirred CH_2Cl_2 solution of **3d** (100 mg, 0.24 mmol) was deprotected using BBr_3 according to the general demethylation procedure. The crude product was purified by flash chromatography (10% CH_3OH/CH_2Cl_2) to afford **4d** as a tan powder (70 mg, 76%): mp 225 °C dec; ^{1}H NMR (MeOD-d_4, 500 MHz) δ 0.63 (d, 6H, J = 6,5), 1.51 (m, 1H, J = 7.0), 2.51 (d, 2H, J = 7.5), 6.76 (AA′XX′, 2H, J = 9.0, 2.3), 6.87 (AA′XX′, 2H, J = 8.9, 2.3), 7.02 (AA′XX′, 2H, J = 8.5, 2.4), 7.26 (m, 5H), 7.49 (AA′XX′, 2H, J = 8.0, 2.3); ^{13}C NMR (MeOD-d_4, 125 MHz) δ 22.8, 29.9, 33.8, 116.4, 116.6, 119.1, 123.0, 126.6, 126.8, 128.4, 129.9, 130.9, 132.9, 141.5, 144.2, 153.4, 158.8, 159.2; FAB-HRMS (M + 1) calcd for $C_{25}H_{25}N_2O_2$ 385.1916, found 385.1916.

4-Butyl-3,5-bis(4-hydroxyphenyl)-1-phenyl-1*H*-pyrazole (4e). A stirred CH_2Cl_2 solution of **3e** (100 mg, 0.24 mmol) was deprotected using BBr_3 according to the general demethylation procedure. The crude product was purified by flash chromatography (30% EtOAc/hexanes) to afford a tan solid. This material was subsequently recrystallized from 5−10% MeOH/CH_2Cl_2 to afford the title compound as small off-white crystals (59 mg, 64%): mp 205.5−207.5 °C; ^{1}H NMR (MeOD-d_4, 400 MHz) δ 0.72 (t, 3H, J = 7.2), 1.16 (sext, 2H, J = 7.2), 1.34 (quint, 2H, J = 7.2), 2.60 (t, 2H, J = 7.2), 4.95 (br s, 2H exchange with D_2O), 6.78 (d, 2H, J = 9.0), 6.91 (d, 2H, J = 8.0), 7.02 (d, 2H, J = 8.8), 7.26 (m, 5H), 7.53 (d, 2H, J = 8.4); ^{13}C NMR (MeOD-d_4, 125 MHz) δ 14.6, 23.9, 24.8, 34.3, 116.8, 116.9, 120.5, 123.2, 126.8, 128.7, 130.3, 131.0, 131.1, 133.1, 141.7, 144.0, 153.3, 159.0, 159.4. Anal. ($C_{25}H_{24}N_2O_2 \cdot 0.1H_2O$) C, H, N.

4-Ethyl-1,3,5-tris(4-hydroxyphenyl)-1*H*-pyrazole (4f). A stirred CH_2Cl_2 solution of **3f** (200 mg, 0.48 mmol) was deprotected using BBr_3 according to the general demethylation procedure. A crude oil was isolated which was triturated with a 10% CH_3OH/CH_2Cl_2 solution from which the desired product precipitated. The white powder was collected by filtration and recrystallized from CH_3OH/CH_2Cl_2 to afford the title compound **4f** (175 mg, 98%): mp 210−215 °C; ^{1}H NMR (MeOD-d_4, 400 MHz): δ 0.96 (t, 3H, J = 7.5) 2.58 (q, 2H, J = 7.5) 6.70 (AA′XX′, 2H, J = 8.8, 2.6), 6.77 (AA′XX′, 2H, J = 8.6, 2.3), 6.87 (AA′XX′, 2H, J = 8.8, 2.3), 7.10 (m, 4H), 7.48 (AA′XX′, 2H, J = 8.6, 2.4); ^{13}C NMR (MeOD-d_4, 100 MHz) δ 14.5, 16.6, 114.8, 114.9, 114.9, 119.2, 121.4, 125.0, 126.8, 129.1, 131.2, 131.9, 142.1, 150.5, 156.7, 157.1, 157.5. Anal. ($C_{23}H_{20}N_2O_3 \cdot 0.7H_2O$) C, H, N.

1,3,5-Tris(4-hydroxyphenyl)-4-propyl-1*H*-pyrazole (4g). A stirred CH_2Cl_2 solution of **3g** (200 mg, 0.48 mmol) was deprotected using BBr_3 according to the general demethylation procedure. A crude oil was isolated which was triturated with a 10% CH_3OH/CH_2Cl_2 solution from which the desired product precipitated. The white powder was collected by filtration and recrystallized from CH_3OH/CH_2Cl_2 to afford the title compound **4g** (125 mg, 68%): mp 230 °C dec; ^{1}H NMR (MeOD-d_4, 400 MHz) δ 0.72 (t, 3H, J = 7.2), 1.33 (sext, 2H, J = 7.6), 2.54 (t, 2H, J = 8), 6.70 (AA′XX′, 2H, J = 8.8, 2.4), 6.76 (AA′XX′, 2H, J = 6.8, 2.0), 6.87 (AA′XX′, 2H, J = 8.8, 2.4), 7.02 (AA′XX′, 2H, J = 8.8, 2.4), 7.05 (AA′XX′, 2H, J = 9.2, 2.4), 7.47 (AA′XX′, 2H, J = 8.8, 2.0); ^{13}C NMR (MeOD-d_4, 100 MHz) δ 25.8 (CH_3), 36.4 (CH_2), 38.4 (CH_2), 127.0 (C), 128.0 (C), 128.5 (C), 130.5 (CH), 134.3 (CH), 137.9 (CH), 138.9 (C), 140.3 (C), 141.3 (C), 142.8 (C), 143.3 (C), 144.1 (C),144.7 (CH), 155.3 (CH), 163.6 (CH), 169.5 (CH), 170.3 (CH). Anal. ($C_{24}H_{22}N_2O_3 \cdot 0.6H_2O$) C, H, N.

4-Isobutyl-1,3,5-tris(4-hydroxyphenyl)-1*H*-pyrazole (4h). A stirred CH_2Cl_2 solution of **3h** (250 mg, 0.56 mmol) was

deprotected using BBr_3 according to the general demethylation procedure. Recrystallization from CH_3OH/CH_2Cl_2 afforded the title compound **4h** as an off-white powder (80 mg, 37%): mp 226−228 °C; ^{1}H NMR (MeOD-d_4, 500 MHz) δ 0.61 (d, 6H, J = 6.5), 1.50 (m, 1H, J = 7.0), 2.50 (d, 2H, J = 7.5), 4.87 (s, 3H, OH), 6.70 (AA′XX′, 2H, J = 8.5, 2.0), 6.75 (AA′XX′, 2H, J = 8.5, 2.3), 6.85 (AA′XX′, 2H, J = 9.0, 2.3), 7.01 (AA′XX′, 2H, J = 9.0, 2.3), 7.05 (AA′XX′, 2H, J = 9.0, 2.3), 7.45 (AA′XX′, 2H, J = 8.5, 2.3); ^{13}C NMR (MeOD-d_4, 125 MHz) δ 22.9, 29.9, 33.9, 116.4, 116.5, 116.6, 118.3, 123.2, 126.9, 128.3, 130.9, 132.9, 133.5, 144.3, 152.7, 158.2, 158.6, 158.9. Anal. ($C_{25}H_{24}N_2O_3$·$0.7H_2O$) C, H, N.

4-Butyl-1,3,5-tris(4-hydroxyphenyl)-1*H*-pyrazole (4i). A stirred CH_2Cl_2 solution of **3i** (200 mg, 0.45 mmol) was deprotected using BBr_3 according to the general demethylation procedure. Recrystallization from CH_3OH/CH_2Cl_2 afforded the title compound **4i** as an off-white powder (90 mg, 50%): mp 214−230 °C dec; ^{1}H NMR (MeOD-d_4, 500 MHz) δ 0.71 (t, 3H, J = 7.5), 1.13 (sext, 2H, J = 7.0), 1.30 (quint, 2H, J = 8.5), 2.57 (t, 2H, J = 8.0), 6.70 (AA′XX′, 2H, J = 9.0, 2.4), 6.76 (AA′XX′, 2H, J = 8.5, 2.3), 6.86 (AA′XX′, 2H, J = 9.0, 2.5), 7.02 (AA′XX′, 2H, J = 8.5, 2.3), 7.05 (AA′XX′, 2H, J = 8.5, 2.3), 7.46 (AA′BB′, 2H, J = 8.5, 2.3); ^{13}C NMR (MeOD-d_4, 400 MHz) δ 14.1, 23.5, 24.4, 33.9, 116.3, 116.4, 116.5, 119.3, 123.0, 126.7, 128.3, 130.7, 132.8, 133.5, 143.9, 152.4, 158.3, 158.7, 159.0. Anal. ($C_{25}H_{24}N_2O_3$·$0.3H_2O$) C, H, N.

4-Isopropyl-3,5-bis(4-methoxyphenyl)-1-phenyl-1*H*-pyrazole (6).[13] Upon solid support cleavage and solvent removal, the crude solid was recrystallized from 25% ethyl acetate/hexane to afford **6** as small cubic crystals (30 mg, 11% over three steps): mp 225−230 °C; ^{1}H NMR (MeOD-d_4, 400 MHz) δ 1.09 (d, 6H, J = 7.0 Hz) 2.98 (septet, 1H, J = 7.11 Hz), 6.76 (AA′XX′, 2H, J = 9.1, 2.6), 6.88 (AA′XX′, 2H, J = 9.0, 2.6), 7.1 (AA′XX′, 2H, J = 8.7, 2.5), 7.20−7.30 (m, 5H), 7.39 (AA′XX′, 2H, J = 8.8, 2.40); ^{13}C NMR (MeOD-d_4, 100 MHz) δ 22.5, 24.5, 114.5, 114.6, 121.6, 124.6, 125.0, 126.7, 128.2, 130.2, 131.8, 139.6, 141.3, 151.3, 157.2, 157.6; HRMS (EI, M^+) calcd for $C_{24}H_{22}N_2O_2$ 370.1681, found 370.1674.

1,3-Bisphenylpropane-1,3-dione (10). To a stirred solution of diketone **9** (2g, 8.9 mmol) in freshly distilled THF (50 mL), was added 8.9 mL (8.9 mmol) of tetrabutylammonium fluoride (1 M in THF) and stirred for 30 min. The solution was concentrated under reduced pressure and dissolved in 50 mL of $CHCl_3$. Ethyl iodide (1.4 mL, 17.8 mmol) was added in one portion and stirred at room temperature overnight. The solution was concentrated and the crude was purified by flash chromatgraphy (petroleum ether/CH_2Cl_2, 1:1) to give 920 mg of **19** as a white solid in 41% yield: ^{1}H NMR ($CDCl_3$, 400 MHz) δ 1.05 (t, 3H, J = 7.4), 2.17 (quint, 2H, J = 7.4), 5.12 (t, 1H, J = 6.5) 7.42−7.58 (m, 6H), 7.94−7.98 (m, 4H); ^{13}C NMR δ 12.8, 22.9, 58.7, 128.5, 128.8, 133.4, 136.1, 196.1; MS (EI, 70 eV) m/z 252.1 (M^+).

4-Ethyl-1-(4-methoxyphenyl)-3,5-bisphenyl-1*H*-pyrazole (11). The diketone **10** (300 mg, 1.2 mmol) was reacted with 4-methoxyphenylhydrazine hydrochloride (830 mg, 4.7 mmol) according to the general procedure for pyrazole synthesis. The crude product was purified by flash chromatography (petroleum ether/CH_2Cl_2, 1:1) to afford 276 mg of **11** as a yellow oil (65%): ^{1}H NMR ($CDCl_3$, 400 MHz) δ 1.04 (t, 3H, J = 7.5), 2.67 (q, 2H, J = 7.5), 3.77 (s, 1H), 6.77 (AA′XX′, 2H, J = 1.0, 2.2), 7.19 (AA′XX′, 2H, J = 9.1, 2.2), 7.23−7.48 (m, 9H), 7.78 (AA′XX′, 2H, J = 8.2, 2.5); ^{13}C NMR δ 15.6, 17.1, 55.4, 113.8, 120.4, 126.1, 127.5, 127.9, 128.1, 128.41, 128.45, 130.1, 130.9, 133.4, 134.1, 141.2, 150.4, 158.2; MS (EI, 70 eV) m/z 354.2 (M^+).

4-Ethyl-1-(4-hydroxyphenyl)-3,5-bisphenyl-1*H*-pyrazole (7a). A stirred CH_2Cl_2 solution of **11** (274 mg, 0.77 mmol) was deprotected with BBr_3 according to the general demethylation procedure. The crude was purified by flash chromatography (CH_2Cl_2/acetone, 3:1) to give 84 mg of **7a** as a white solid (32%): mp 184−185 °C; ^{1}H NMR (CD_3OD, 400 MHz) δ 1.03 (t, 3H, J = 7.5), 2.66 (q, 2H, J = 7.5), 6.65 (AA′XX′, 2H J = 8.8, 2.2), 7.09 (AA′XX′, 2H, J = 9.0, 2,1), 7.2−7.5 (m, 8H), 7.77 (AA′XX′, 2H, J = 8.4); ^{13}C NMR δ 15.5, 17.0, 115.8, 120.2, 126.6, 127.7, 128.0, 128.2, 128.4, 128.5, 130.0, 130.6, 132.6, 133.8, 141.6, 150.5, 155.2; MS (EI, 70 eV) m/z 340.2 (M^+). Anal. ($C_{23}H_{20}ON_2$) C, H, N.

1,3-Bis(4-methoxyphenyl)-5-phenyl-4,5-dihydro-1*H*-pyrazole (13a). A mixture of commercially available 4′-methoxychalcone (**12a**; 253 mg, 1.1 mmol) and 807 mg of 4-methoxyphenylhydrazine (4.6 mmol) in 10 mL of anhydrous DMF was heated to 85 °C overnight. The reaction solution was cooled to room temperature and partitioned with diethyl ether and water. The organic layer was washed with water, dried ($MgSO_4$), and concentrated. The crude was then recrystallized from a mixture of ethyl acetate and hexanes to give 198 mg of **13a** as light yellow crystals (48%): ^{1}H NMR ($CDCl_3$, 400 MHz) δ 3.12 (dd, 1H, J = 16.7, 8.4), 3.74 (s, 3H), 3.86 (s, 3H), 3.74−3.88 (m, 1H), 5.14 (dd, 1H, J = 11.9, 8.6), 6.8 (AA′XX′, 2H, J = 9.0), 6.94 (AA′XX′, 2H, J = 9.0), 7.04 (AA′XX′, 2H, J = 9.0), 7.26−7.42 (m, 5H), 7.68 (d, 2H, J = 9.0); ^{13}C NMR δ 43.9, 55.3, 55.6, 65.8, 114.0, 114.4, 114.8, 126.1, 127.5, 127.8, 128.0, 129.1, 140.1, 142.9, 146.9, 153.2, 160.0; HRMS (EI, M^+) calcd for $C_{23}H_{22}N_2O_2$ 358.1688, found 358.1681.

1,5-Bis(4-methoxyphenyl)-3-phenyl-4,5-dihydro-1*H*-pyrazole (13b). A mixture of commercially available 4-methoxychalcone (**12b**; 2 g, 8.4 mmol) and 7.3 g of 4-methoxyphenylhydrazine (42 mmol) in 80 mL of anhydrous DMF was heated to 85 °C overnight. The reaction solution was cooled to room temperature and partitioned with diethyl ether and water. A yellow solid precipitated and was collected by filtration to give 2.6 g of **13b** (86%): ^{1}H NMR ($CDCl_3$, 400 MHz) δ 3.1 (dd, 1H, J = 15.6,7.8), 3.72 (s, 3H), 3.78 (s, 3H), 3.8 (d, 1H, J = 5.6), 5.13 (dd, 1H, J = 12.0, 9.0), 6.76 (AA′XX′, 2H, J = 9.1, 2.3), 6.87 (AA′XX′, 2H, J = 8.7, 2.1), 7.01 (d, 2H, J = 9.0), 7.2−7.4 (m, 5H), 7.7 (d, 2H, J = 7.3); ^{13}C NMR δ 43.7, 55.2, 55.6, 65.2, 114.4, 114.4, 114.9, 125.6, 127.3, 128.3, 128.5, 132.9, 134.7, 139.7, 146.3, 153.3, 158.9; MS (EI, 70 eV) m/z 358.2 (M^+).

4-Ethyl-1,3-bis(4-methoxyphenyl)-5-phenyl-4,5-dihydro-1*H*-pyrazole (14a). To a solution of lithium diisopropylamide in 20 mL of THF [prepared by dropwise addition of 0.88 mL of *n*-BuLi (1.41 mmol) to 0.21 mL (1.5 mmol) of diisopropylamine in 18 mL of THF at −78 °C] was added a solution of 317 mg (0.88 mmol) of pyrazoline **13a** in 8 mL of THF dropwise via syringe at −78 °C and stirred for 1 h. To the dark red solution was added iodoethane (0.11 mL, 1.31 mmol) in one portion and the resulting yellow solution was warmed to room temperature overnight. The reaction was quenched with 5 mL of brine, the aqueous layer was separated and extracted with CH_2Cl_2, the organic layer was dried ($MgSO_4$) and concentrated in vacuo. The residue was purified by flash chromatography (ether/hexanes, 3:2) to afford 262 mg of **14a** as a yellow foam (77%): ^{1}H NMR ($CDCl_3$, 400 MHz) δ 0.8 (t, 3H, J = 7.3), 1.45 (tq, 1H, J = 4, 2), 1.55 (m, 1H), 3.2 (m, 1H), 3.25 (s, 3H), 3.3 (s, 3H), 4.8 (d, 1H, 3.4), 6.77 (AA′XX′, 2H, J = 8.9), 6.82 (AA′XX′, 2H, J = 8.5), 7.0 (AA′XX′, 2H, J = 8.7), 7.13 (AA′XX′, 2H, J = 8.5), 7.25−7.40 (m, 3H), 7.70 (AA′XX′, 2H, J = 7.3); ^{13}C NMR δ 10.5, 25.4, 54.8, 55.1, 57.8, 69.7, 114.4, 114.4, 115.0, 125.8, 126.0, 127.5, 127.7, 129.3, 139.3, 142.8, 148.4, 153.6, 160.2; HRMS (EI, M^+) calcd for $C_{25}H_{26}N_2O_2$ 386.1999, found 386.1994.

4-Ethyl-1,5-bis(4-methoxyphenyl)-3-phenyl-4,5-dihydro-1*H*-pyrazole (14b). Prepared from lithium diisopropylamide (4.65 mmol), pyrazoline **13b** (1 g, 2.8 mmol), and ethyl iodide (0.45 mL, 5.6 mmol) by the procedures used to prepare pyrazoline **14a**. The crude product was purified by flash chromatography (hexanes/ether 3:2) to give 0.33 g (38%) of **14b** a yellow foam: ^{1}H NMR ($CDCl_3$, 400 MHz) δ 1.03 (t, 3H, J = 7.3), 1.69 (tq, 1H, J = 4, 2), 1.85 (m, 1H), 3.37 (m, 1H), 3.73 (s, 3H), 3.75 (s, 3H), 4.91 (d, 1H, 3.4), 6.77 (AA′XX′, 2H, J = 8.9), 6.82 (AA′XX′, 2H, J = 8.5), 7.0 (AA′XX′, 2H, J = 8.7), 7.13 (AA′XX′, 2H, J = 8.5), 7.25−7.40 (m, 3H), 7.70 (AA′XX′, 2H, J = 7.3); ^{13}C NMR δ 10.5, 25.1, 55.2, 55.6, 57.3, 68.9, 113.9, 114.4, 114.5, 125.8, 126.8, 127.9, 128.5, 132.6, 134.1, 138.5, 148.5, 152.8, 158.8; MS (EI, 70 eV) m/z 386.2 (M^+).

4-Ethyl-1,3-bis(4-methoxyphenyl)-5-phenyl-1*H*-pyrazole (15a). To a stirred solution of **14a** (27.8 mg, 0.07 mmol)

in 3 mL of benzene was added 78 mg (0.9 mmol) of MnO_2. The solution was heated to 100 °C with a Dean−Stark trap for 2 h, cooled to room temperature, filtered through Celite and concentrated. The crude was chromatographed (EtOAc/hexanes, 1:10) to afford 28 mg of **15a** (100%): ^{1}H NMR ($CDCl_3$, 400 MHz) δ 1.12 (t, 3H, J = 7.5), 2.65 (q, 2H, J = 7.5), 3.78 (s, 3H), 3.85 (s, 3H), 6.77 (AA′XX′, 2H, J = 9.0, 2.0), 7.0 (AA′XX′, 2H, J = 8.8, 2.0), 7.2 (AA′XX′, 2H, J = 9.0, 2.0), 7.22−7.40 (m, 5H), 7.71 (d, 2H, J = 8.6, 2.0); ^{13}C NMR δ15.5, 17.1, 55.2, 55.4, 113.8, 113.8, 120.1, 126.1, 126.8, 128.1, 128.4, 129.1, 130.1, 131.1, 133.5, 141.1, 150.2, 158.2, 159.1; HRMS (EI, M^+) calcd for $C_{25}H_{24}N_2O_2$ 385.1912, found 385.1916.

4-Ethyl-1,5-bis(4-methoxyphenyl)-3-phenyl-1*H*-pyrazole (15b). A mixture of 147 mg (0.37 mmol) of pyrazoline **14b** and 127 mg (0.56 mmol) of dichlorodicyanoquinone in 10 mL of benzene was heated to reflux for 5 h. The mixture was cooled to room temperature and filtered through a plug of Celite with diethyl ether. The filtrate was concentrated in vacuo and the residue was chromatographed (hexanes/ethyl acetate, 4:6) to give 130 mg (90%) of **15b** as a white solid: ^{1}H NMR ($CDCl_3$, 400 MHz) δ 1.04 (t, 3H, J = 7.5), 2.65 (q, 2H, J = 7.5), 3.78 (s, 3H), 3.83 (s, 3H), 6.79 (AA′XX′, 2H, J = 8.9, 2.0), 6.89 (AA′XX′, 2H, J = 8.5, 2.0), 7.16 (AA′XX′, 2H, J = 8.3, 1.8), 7.20 (AA′XX′, 2H, J = 8.7, 2.1), 7.3−7.5 (m, 3H), 7.77 (AA′XX′, 2H, J = 8.8, 1.8); ^{13}C NMR δ 15.6, 17.12, 55.2, 55.4, 113.7, 113.9, 120.2, 123.2, 126.1, 127.4, 127.9, 128.4, 131.3, 133.5, 134.27, 141.07, 150.3, 158.1, 159.3; MS (EI, 70 eV) m/z 384.2 (M^+).

4-Ethyl-1,3-bis(4-hydroxyphenyl)-5-phenyl-1*H*-pyrazole (8a). A stirred CH_2Cl_2 solution of **15a** (26 mg, 0.068 mmol) was deprotected with BBr_3 according to the general demethylation procedure. The crude was purified by flash chromatography (CH_2Cl_2/MeOH, 10:1) to give 17 mg of **8a** as a tan solid (70%): mp 225−227 °C; ^{1}H NMR (CD_3OD, 500 MHz) δ 0.8 (t, 3H, J = 7.5), 2.5 (q, 2H, J = 7.5), 6.58 (AA′XX′, 2H, J = 9.0, 2.2), 6.78 (AA′XX′, 2H, J = 8.5, 2.0), 6.94 (AA′XX′, 2H, J = 8.9, 2.0), 7.1−7.3 (m, 5H), 7.39 (AA′XX′, 2H, J = 8.9, 2.0); ^{13}C NMR δ 15.8, 17.9, 116.3, 116.4, 121.0, 122.6, 128.2, 128.9, 129.3, 129.6, 132.6, 133.2, 135.3, 143.8, 151.7, 158.2, 159.0; HRMS (EI, M^+) calcd for $C_{23}H_{20}N_2O_2$ 356.1598, found 356.1603.

4-Ethyl-1,5-bis(4-hydroxyphenyl)-3-phenyl-1*H*-pyrazole (8b). A stirred CH_2Cl_2 solution of **15b** (130 mg, 0.34 mmol) was deprotected with BBr_3 according to the general demethylation procedure. The crude was purified by flash chromatography (CH_2Cl_2/acetone, 3:1) to give 42 mg of **8b** as a white solid (35%): mp 225−226 °C; ^{1}H NMR (CD_3OD, 500 MHz) δ 0.96 (t, 3H, J = 7.5), 2.62 (q, 2H, J = 7.5), 6.71 (AA′XX′, 2H, J = 9.1, 2.2), 6.77 (AA′XX′, 2H, J = 8.5, 2.0), 7.06 (AA′XX′, 2H, J = 8.9, 2.1), 7.07 (AA′XX′, 2H, J = 9.1, 2.2), 7.35−7.47 (m, 3H), 7.67 (AA′XX′, 2H, J = 8.9, 2.0); ^{13}C NMR δ 15.8, 17.9, 116.3, 116.4, 121.0, 122.6, 128.2, 128.9, 129.3, 129.6, 132.6, 133.2, 135.3, 143.8, 151.7, 158.2, 159.0; HRMS (EI, M^+) calcd for $C_{23}H_{20}N_2O_2$ 356.151939, found 356.152478 Anal. ($C_{23}H_{20}N_2O_2$·0.75H_2O) C, H, N.

Acknowledgment. We are grateful for support of this research through grants from the U.S. Army Breast Cancer Research Program (DAMD17-97-1-7076 to J.A.K.) and the National Institutes of Health (PHS 5R37 DK15556 to J.A.K. and PHS 5R37 CA18119 to B.S.K.). We thank Dr. Ying R. Huang for the preparation of some compounds used in this study. NMR spectra were obtained at the Varian Oxford Instrument Center for Excellence in NMR Laboratory. Funding for this instrumentation was provided in part from the W. M. Keck Foundation and the National Science Foundation (NSF CHE 96-10502). Mass spectra were obtained on instruments supported by grants from the National Institute of General Medical Sciences (GM 27029), the National Institute of Health (RR 01575), and the National Science Foundation (PCM 8121494).

References

(1) Gao, H.; Katzenellenbogen, J. A.; Garg, R.; Hansch, C. Comparative QSAR Analysis of Estrogen Receptor Ligands. *Chem. Rev.* **1999**, *99*, 723−744.
(2) Grese, T. A.; Dodge, J. A. Selective Estrogen Receptor Modulators (SERMs) [Review]. *Curr. Pharm. Des.* **1998**, *4*, 71−92.
(3) Anstead, G. M.; Carlson, K. E.; Katzenellenbogen, J. A. The estradiol pharmacophore: ligand structure-estrogen receptor binding affinity relationships and a model for the receptor binding site. *Steroids* **1997**, *62*, 268−303.
(4) Brzozowski, A. M.; Pike, A. C.; Dauter, Z.; Hubbard, R. E.; Bonn, T.; Engström, O.; Öhman, L.; Greene, G. L.; Gustafsson, J.-A.; Carlquist, M. Molecular basis of agonism and antagonism in the oestrogen receptor. *Nature* **1997**, *389*, 753−758.
(5) Ekena, K.; Weis, K. E.; Katzenellenbogen, J. A.; Katzenellenbogen, B. S. Different residues of the human estrogen receptor are involved in the recognition of structurally diverse estrogens and antiestrogens. *J. Biol. Chem.* **1997**, *272*, 5069−5075.
(6) Shiau, A. K.; Barstad, D.; Loria, P. M.; Cheng, L.; Kushner, P. J.; Agard, D. A.; Greene, G. L. The structural basis of estrogen receptor/coactivator recognition and the antagonism of this interaction by tamoxifen. *Cell* **1998**, *95*, 927−937.
(7) Anstead, G. M.; Peterson, C. S.; Katzenellenbogen, J. A. Hydroxylated 2,3-diarylindenes: Synthesis, estrogen receptor binding affinity, and binding orientation considerations. *J. Steroid Biochem.* **1989**, *33*, 877−887.
(8) Kuiper, G. G. J. M.; Enmark, E.; Pelto-Huikko, M.; Nilsson, S.; Gustafsson, J. Å. Cloning of a novel receptor expressed in rat prostate and ovary. *Proc. Natl. Acad. Sci. U.S.A.* **1996**, *93*, 5925−5930.
(9) Mosselman, S.; Polman, J.; Dijkema, R. ERβ: identification and characterization of a novel human estrogen receptor. *FEBS Lett.* **1996**, *392*, 49−53.
(10) Kuiper, G. G. J. M.; Carlsson, B.; Grandien, K.; Enmark, E.; Häggblad, J.; Nilsson, S.; Gustafsson, J.-Å. Comparison of the ligand binding specificity and transcript tissue distribution of estrogen receptor α and β. *Endocrinology* **1997**, *138*, 863−870.
(11) Fink, B. E.; Mortensen, D. S.; Stauffer, S. R.; Aron, Z. D.; Katzenellenbogen, J. A. Novel Structural Templates for Estrogen-Receptor Ligands and Prospects for Combinatorial Synthesis of Estrogens. *Chem. Biol.* **1999**, *6*, 205−219.
(12) Katzenellenbogen, J. A.; Katzenellenbogen, B. S.; Fink, B. S.; Stauffer, S. R.; Mortensen, D. S.; Sattigeri, V. J.; Huang, Y. Estrogen Receptor Ligands. Patent WO 00/19994, Apr 13, 2000.
(13) Stauffer, S. R.; Katzenellenbogen, J. A. Solid-Phase Synthesis of Tetrasubstituted Pyrazoles, Novel Ligands for the Estrogen Receptor. *J. Comb. Chem.* **2000**, *2*, 318−329.
(14) Sun, J.; Meyers, M. J.; Fink, B. E.; Rajendran, R.; Katzenellenbogen, J. A.; Katzenellenbogen, B. S. Novel Ligands that Function as Selective Estrogens or Antiestrogens for Estrogen Receptor-α or Estrogen Receptor-β. *Endocrinology* **1999**, *140*, 800−804.
(15) Huang, Y.; Katzenellenbogen, J. A. Regioselective synthesis of 1,3,5-triaryl-4-alkylpyrazoles: Novel ligands for the estrogen receptor. *Org Lett.* **2000**, *2*, 2833−2836.
(16) Carlson, K. E.; Choi, I.; Gee, A.; Katzenellenbogen, B. S.; Katzenellenbogen, J. A. Altered ligand binding properties and enhanced stability of a constitutively active estrogen receptor: Evidence that an open pocket conformation is required for ligand interaction. *Biochemistry* **1997**, *36*, 14897−14905.
(17) Meyers, M. J.; Sun, J.; Carlson, K. E.; Katzenellenbogen, B. S.; Katzenellenbogen, J. A. Estrogen receptor subtype-selective ligands: Asymmetric synthesis and biological evaluation of *cis*- and *trans*-5,11-dialkyl-5,6,11,12-tetrahydrochrysenes. *J. Med. Chem.* **1999**, *42*, 2456−2468.
(18) We are grateful to a referee for noting this relationship.
(19) Grese, T. A.; Cho, S.; Finley, D. R.; Godfrey, A. G.; Jones, C. D.; Lugar, C. W., III; Martin, M. J.; Matsumoto, K.; Pennington, L. D.; Winter, M. A.; Adrian, M. D.; Cole, H. W.; Magee, D. E.; Phillips, D. L.; Rowley, E. R.; Short, L. L.; Glasebrook, A. L.; Bryant, H. U. Structure−activity relationships of selective estrogen receptor modulators: Modifications at the 2-arylbenzothiophene core of raloxifene. *J. Med. Chem.* **1997**, *40*, 146−167.
(20) Pons, M.; Michel, F.; Crastes de Paulet, A.; Gilbert, J.; Miquel, J.-F.; Precgoux, G.; Hospital, M.; Ojasoo, T.; Raynaud, J.-P. Influence of new hydroxylated triphenylethylene (TPE) derivatives on estradiol binding to uterine cytosol. *J. Steroid Biochem.* **1984**, *20*, 137−145.
(21) Katzenellenbogen, J. A.; O'Malley, B. W.; Katzenellenbogen, B. S. Tripartite steroid hormone receptor pharmacology: Interaction with multiple effector sites as a basis for the cell- and promoter-specific action of these hormones. *Mol. Endocrinol.* **1996**, *10*, 119−131.

(22) Kraichely, D. M.; Sun, J.; Katzenellenbogen, J. A.; Katzenellenbogen, B. S. Conformational Changes and Coactivator Recruitment by Novel Ligands for Estrogen Receptor-α and Estrogen Receptor-*β*: Correlations with Biological Character and Distinct Differences among SRC Coactivator Family Members. *Endocrinology* **2000**, *141*, 3534.
(23) Stauffer, S. R.; Huang, Y.; Coletta, C. J.; Katzenellenbogen, J. A. Estrogen Pyrazoles: Defining the Pyrazole Core Structure and Orientation of Substituents in the Ligand Binding Pocket of the Estrogen Receptor. *Biorg. Med. Chem.* **2000**, in press.
(24) Stauffer, S. R.; Huang, Y.; Aron, Z. D.; Coletta, C. J.; Sun, J.; Katzenellenbogen, B. S.; Katzenellenbogen, J. A. Triarlpyrazoles with basic side chains: Development of pyrazole-based estrogen receptor antagonists. *Biorg. Med. Chem.* **2000**, in press.
(25) Pike, A. C.; Brzozowski, A. M.; Hubbard, R. E.; Bonn, T.; Thorsell, A. G.; Engstrom, O.; Ljunggren, J.; Gustafsson, J.; Carlquist, M. Structure of the ligand-binding domain of oestrogen receptor beta in the presence of a partial agonist and a full antagonist. *EMBO J.* **1999**, *18*, 4608−4618.
(26) Still, W. C.; Kahn, M.; Mitra, A. Rapid chromatographic technique for preparative separations with moderate resolution. *J. Org. Chem.* **1978**, *43*, 2923−2926.
(27) Hachiya, I.; Moriwaki, M.; Kobayashi, S. Hafnium (IV) Trifluoromethanesulfonate, An Efficient Catalyst for the Friedel−Crafts Acylation and Alkylation Reactions. *Bull. Chem. Soc. Jpn.* **1995**, *68*, 2053−2060.
(28) Wang, D.; Chen, D.; Haberman, J.; Li, C. J. Ruthenium-Catalyzed Isomerization of Homoallylic Alcohols in Water. *Tetrahedron* **1998**, *54*, 5129−5142.
(29) Horiuchi, Y.; Oshima, K.; Utimoto, K. Titanium Tetrachloride-Induced Three-Component Coupling Reaction of α-Haloacylsilane, Allysilane, and Carbonyl Compound. *J. Org. Chem.* **1996**, *61*, 4483−4486.
(30) Narasaka, K.; Kusama, H. Friedel−Crafts Acylation of Arenes Catalyzed by Bromopentacarbonylrhenium (I). *Bull. Chem. Soc. Jpn.* **1995**, *68*, 2379−2383.
(31) Williams, D.; Gorski, J. Equilibrium binding of estradiol by uterine cell suspensions and whole uteri in vitro. *Biochemistry* **1974**, *13*, 5537−5542.
(32) McInerney, E. M.; Tsai, M. J.; O'Malley, B. W.; Katzenellenbogen, B. S. Analysis of estrogen receptor transcriptional enhancement by a nuclear hormone receptor coactivator. *Proc. Natl. Acad. Sci. U.S.A.* **1996**, *93*, 10069−10073.
(33) Katzenellenbogen, J. A.; Johnson, H. J., Jr.; Myers, H. N. Photoaffinity labels for estrogen binding proteins of rat uterus. *Biochemistry* **1973**, *12*, 4085−4092.

JM000170M